Review

Not peer-reviewed version

Review of Measuring Methods of Residual Stress in Wire Arc Additive Manufacturing Products

Fakada Dabalo Gurmesa *, Hirpa Gelgele Lemu *, Yosef Wakjira Adugna, Mesfin Demise Harsibo

Posted Date: 8 May 2024

doi: 10.20944/preprints202405.0422.v1

Keywords: residual stress; Wire Arc Additive Manufacturing; process parameters; residual stress measurement; wire arc additive manufacturing assessment

Review

Review of Measuring Methods of Residual Stress in Wire Arc Additive Manufacturing Products

Fakada Dabalo Gurmesa [1,*], Hirpa Gelgele Lemu [2,*], Yosef Wakjira Adugna [2] and Mesfin Demise Harsibo [3]

[1] Faculty of Mechanical Engineering, Jimma Institute of Technology, Jimma University, P.O. Box 378, Ethiopia
[2] Department of Mechanical and Structural Engineering and Materials Science, Faculty of Science and Technology, University of Stavanger, N-4036 Stavanger, Norway; yosef.w.adugna@uis.no
[3] Department of Mechanicanical Engineering, College of Engineering and Technology, Wolkite University, P.O. Box 07, Ethiopia; mesfine2021@gmail.com
* Correspondence: fd.gurmesa@stud.uis.no (F.D.G.); hirpa.g.lemu@uis.no (H.G.L.)

Abstract: This literature review provides an in-depth exploration of the research conducted on the investigation and measurement of residual stress (RS) in Wire Arc Additive Manufacturing (WAAM) products, particularly focusing on how process parameters influence the phenomenon. RS plays a crucial role in determining the mechanical behavior and structural integrity of WAAM components. This review article gives an understanding of the relationship between process parameters and RS to optimize the WAAM processes and ensure the durability of the final products. It also summarizes key findings, measurement techniques, challenges, and future directions in this evolving field. The review also analyzes a measurement of RS in the products of WAAM as a function of process parameters depending on examining various research studies, techniques, and methodologies employed in their studies. Experimental measuring techniques and numerical analysis of RS to determine the impacts of RS in mechanical response in products of WAAM were discussed. By offering a comprehensive overview of current research trends and insights, this review serves as a valuable resource to guide future investigations, fostering the advancement of WAAM as a robust and efficient manufacturing technology.

Keywords: residual stress; wire arc additive manufacturing; process parameters; residual stress measurement; wire arc additive manufacturing assessment

1. Introduction

Wire Arc Additive Manufacturing (WAAM) is an advanced manufacturing process that is categorized as additive manufacturing (AM) or 3D printing. It is the imperative metal manufacturing process for large and complex components using wire metals or alloys as feedstock. In addition, due to its fast build-up rates metallurgical characteristics of WAAM fabricated parts are better than those of other AM techniques [1–3]. An important aspect that still hinders this technology is standardization and certification within nondestructive testing of the parts, which is discussed in the literature [4]. In this context, there are no standards for WAAM systems and no in-situ observing, and monitoring techniques for any instant formation of defects (residual stress) that can be fixed after its formation, which leads to waste the materials and time for reproduction. WAAM is an innovative and versatile 3D printing technology with an extensive variety of applications and several advantages in manufacturing.

Early investigations suggest that the adoption of AM technologies in construction could potentially lower labor expenses, diminish material waste, and fabricate intricate custom shapes that typically challenge the manufacturer using conventional construction techniques [5–7]. However, the WAAM sector is interested in large-scale with high deposition rates of AM for producing components spanning from hundreds of millimeters to meters in size [8]. It harvests substantial attention in

 doi:10.20944/preprints202405.0422.v1

industrial manufacturing due to its cost-reliable fabrication of large-scale metal parts at high deposition rates [9]. Besides, Williams et al. [10] suggest that WAAM is a viable contender for substituting the existing manufacturing approach involving solid billets or extensive forgings, particularly for low to medium-complexity components.

Within the context of WAAM products, the presence of RS and deformations due to process parameters becomes a significant issue as they have a substantial impact on the quality, cost, and precision of the printing process [11–13]. Additionally, WAAM, which is a subset of AM, is getting significant interest from all researchers because of its various benefits, including its ability to achieve high metal deposition rates and produce near-net shapes, surpassing conventional manufacturing methods with its higher thermal residual stresses (RS) [3,14–16]. It is an emerging metal additive manufacturing technique, that is gradually providing a competitive edge over traditional forging and casting methods [17]. Depending on the heat sources, the WAAM process is categorized into three; namely inert gas welding, metal arc welding, and plasma arc [18,19].

The need and purpose of this review article is to investigate measurement techniques of RS in the products of WAAM. Notably, this review is essential to gain a deep comprehension of how RS is distributed in the products of WAAM and how it correlates with the deposition parameters. In this study, methods of examining and measuring RS, the impact of RS on material characteristics of WAAM products, and process parameters based on both experimental and numerical analysis were discussed, while the mitigation of the RS and refining grain structure of created layer parts improved based on the experimental methods was discussed. In this review, the effects of process parameters like wire diameter, scan length with width, height (thickness) of bead, arc current behavior [20], voltage, travel speed, welding sequence (welding position) [21], types of shield gas, and its flow rate on RS are considered. Also, studies on the consequence of interlayer bead surface condition and inter pass time on the deposit shape additively increased height were considered.

This review also primarily focuses on how to measure RS fabricated with WAAM, drawing upon pertinent data from existing literature. The techniques for measuring RS through experimental approaches are mostly neutron diffraction [22–24], and X-ray diffraction (XRD) [25–27] that are performed within limited layer depth of printed products. Other methods like the hole-drilling strain gauge method, ultrasonic stress measurement (USM), Barkhausen noise analysis, layer removal (deep hole drilling), contour method, and incremental hole-drilling technique have been employed, and some of them have not been used yet. Importantly, this review explicitly delineates those that have been used and those that have not.

The format of the article is as follows: after this introductory section, Section 2 provides details about the materials and methods used in the research. This is followed by Sections 3 and 4, which respectively present an overview of the products of WAAM and discuss the impact of RS affecting the mechanical attributes of WAAM components. Section 5 focuses on explaining the mitigation strategies for RS and explores practical applications. Section 6 serves as a discussion section, offering a detailed analysis and interpretation of the findings. Lastly, Section 7 summarizes the article by outlining the key points and providing insights into future research directions.

2. Materials and Methods

This review focuses on the scientific literature published within the last ten years, which encompasses open-access sources primarily published between 2015 and 2024. To ensure comprehensive coverage of related research, the investigation targets the defects mainly on the RS of the WAAM products based on the many process and operational parameters. To achieve the aim of this review article, the review concentrates on the latest publications (as indicated based on the data given in Figure 1), with content thematically arranged around specific issues. The search was restricted to sources that have exclusively available articles published in English. It includes articles in the following scientific databases: scientific.net, Scopus, Elsevier, Science Direct, Web of Science, Compendia, Google Scholar, IEEE Xplore, ProQuest, ASM Digital Library, SpringerLink, Mendeley and ResearchGate, semantic scholar, SCISPACE, PubMed, DOAJ, JSTOR, MPDI, BASE, SAGE, Taylor & Francis and others. It employed the English expression to search terms such as AM, WAAM, RS

 doi:10.20944/preprints202405.0422.v1

measurement, process parameters analysis, quality assessment in WAAM, WAAM product defects, characterization of microstructure in WAAM products, WAAM quality control, WAAM RS investigation, and frequently utilized additional descriptive terms to align with the review's objectives precisely. To accomplish these statistical combination and analysis of data from multiple studies to draw overall conclusions.

To screen the retrieved articles from the sources, the advanced text-mining techniques allowed for the finding of significant relations between keywords and the detection of groups of related terms in the gathered publications. For the research explored various RS measuring methods in WAAM components, some articles modeled bead formation during the WAMM process related to process parameters results for different levels of RS. The assessed number of research fields of RS in WAAM is shown in Figure 1 by the statistical analysis that began by examining the yearly count of research publications. Recently, there has been a noticeable increase in research interest in RS in WAAM parts, reflected by the rising number of publications in this domain. A high citation count usually indicates the influential nature of these findings, implying that they establish fundamental knowledge or introduce groundbreaking results that inspire and impact the necessity of the study area.

For the chosen topic, the main strategy used to screen from the retrieved articles is 691, and finally, the total number of articles that passed the screening (included in this article) is 215 as shown in Figure 2. The inclusion criteria utilized were: (1) any WAAM processes and (2) no restriction regarding existing defects in WAAM products for publication years between 2015, and 20224 up to date. The criteria for inclusion and exclusion are outlined as follows: (1) identification through a database, and other sources like libraries; (2) screening for records included and excluded depending on relevant study for the topic with data that is inconsistently extracted, duplicated, or overlaps with other data; (3) eligibility-only papers focused on RS analysis and related; (4) number of articles included with available for RS measurements using experimental and numerical analysis. The flow diagram used for screening and selection studies is depicted in Figure 2.

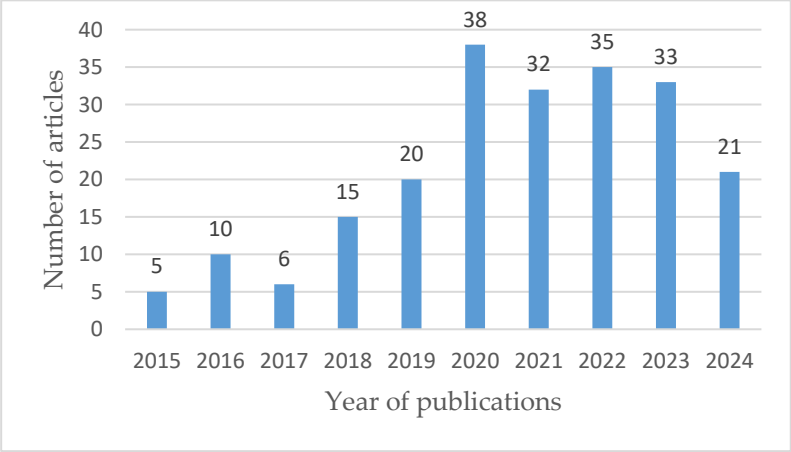

Figure 1. Statistical data on the reviewed articles of a WAAM process publication from 2015 to 2024.

 doi:10.20944/preprints202405.0422.v1

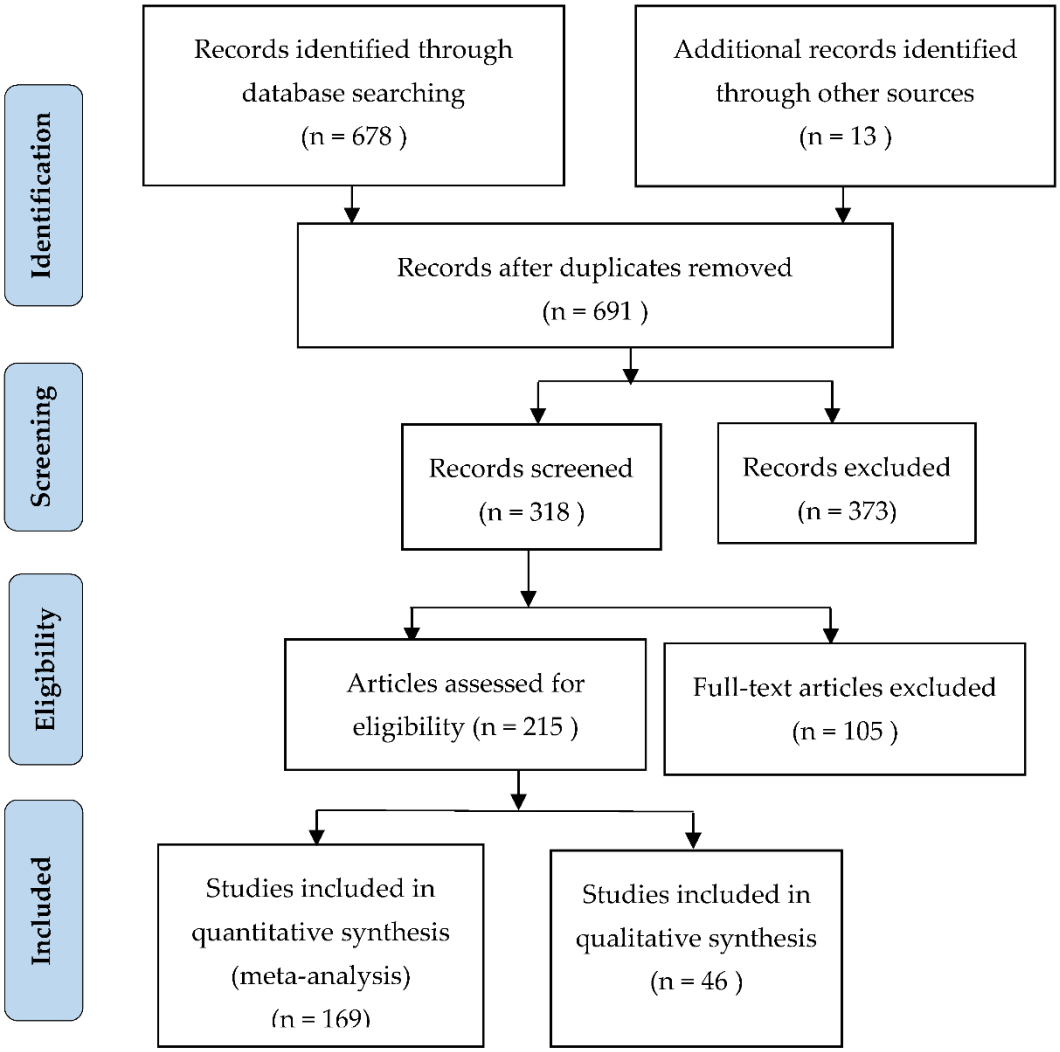

Figure 2. Flow diagram illustrating the screening and selection process of studies.

3. Overview of WAAM of Process and Products

In this technology, large and complex components are made from multiple materials, with a rapid deposition rate, a feat that is challenging to accomplish with traditional AM methods [28, 29]. In this case, wire is supplied to the welding torch and melted by an electric arc [30]. Either robotic or computerized numerical control gantries are used to set the motion of the printing process layer by layer up to the aspired appearance of the components obtained [31]. The 3D digital model serves as the blueprint for this WAAM process. Utilizing robotic guidance in WAAM allows a potent blend of automation and design flexibility, coupled with efficient production processes. However, the material characteristics response of WAAMed products is influenced by both automated robots and computerized numerical control to build up the parts and the associated heat input [32].

Basically, the steps used for the printing process in WAAM products encompass many activities in each stage starting from the CAD model. These steps outline the general workflow for producing components using WAAM, ensuring efficient and reliable manufacturing of complex metal parts. The process of WAAM will be divided into six primary stages from CAD file preparation to component separation to post-processing [31]. The procedure planning steps used for WAAM to produce components are shown in Figure 3.

 doi:10.20944/preprints202405.0422.v1

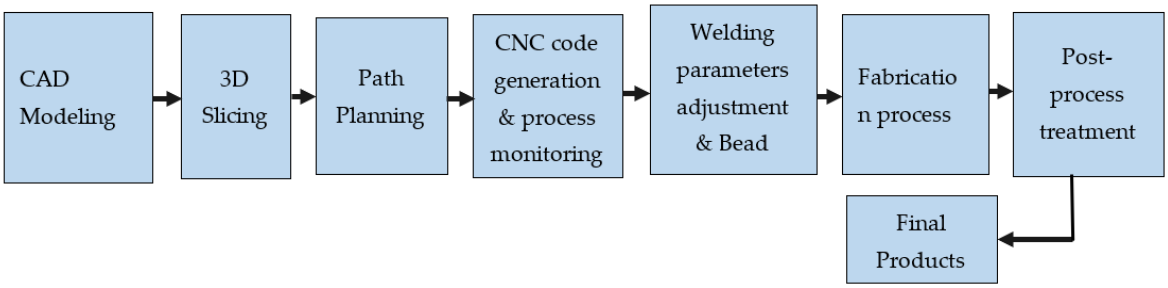

Figure 3. Steps used for WAAM to produce components.

In essence, the RS is inherent in WAAM components due to the various process parameters that can adversely impact the mechanical properties, fatigue life, and structural integrity of the parts. Additionally, assessing RS in WAAM structures is challenging, either due to being laborious and time-intensive or because it lacks the necessary precision [33]. The significance of understanding RS in WAAM products is critical for maintaining structural integrity to address premature failure and ensure the products' mechanical performance [18,34]. The characteristics of the deposited materials may vary through the WAAM process, affecting the evolution of RS [35], as a result of the heat-affected zone (HAZ) in the vicinity of the weld pool [36]. RS measuring also helps in understanding, predicting, and correcting dimensional inaccuracies caused by distortions, ensuring that WAAM products meet desired tolerances [37,38]. Likewise, accurate knowledge of RS is important to enhance product quality and ensure WAAM components meet their performance. By reducing the risk of defects, failures, rework, and/or remanufacture, it can lower production costs and minimize material waste [37,39,40].

WAAM can be utilized for repairing and restoring damaged or worn components and extending the lifespan of expensive equipment and machinery [41,42]. Furthermore, it is highly capable of building large and/or complex metal structures with cost-effective, primarily as a result of its superior deposition rate [3,7,30,43–48]. WAAM is well-suited for creating sizable metallic parts and holds potential for use in the construction industry among various AM methods [20]. The main advantages of these manufacturing methods include their productivity, suitability for industrial applications, and the capacity to decrease material waste compared to other AM techniques [49,50].

3.1. A Robotic System for WAAM

Robotic systems play an important role in WAAM processes, providing versatility and automation that enable precise control over deposition parameters and the capacity to manage intricate geometries [51,52]. These systems incorporate advanced sensors and automation technology to monitor and adjust printing parameters in real-time, ensuring consistent quality and precise deposition of materials. The study reported in [53] concentrated on two WAAM, parameters, namely (1) the speed of wire feed and (2) the robot's movement speed, and investigated their effects on the metallurgical, dimensional stability, and mechanical characteristics of materials. The study involved the production of fine-walled 308L stainless steel parts utilizing the WAAM system, conducted in two steps. Firstly, the effect of welding current, voltage, and travel speed on the shape of individual weld beads was examined, and these factors were fine-tuned for the construction of 308L steel walls. Secondly, a comprehensive analysis was carried out on the influence of the microstructure and mechanical characteristics of the WAAM 308L steel walls, resulting in improved mechanical properties suitable for industrial applications. Robotic components for the printing process with the path of indentation (a), the setup for experimentation (b), and the deposition tool path are illustrated in Figure 4.

 doi:10.20944/preprints202405.0422.v1

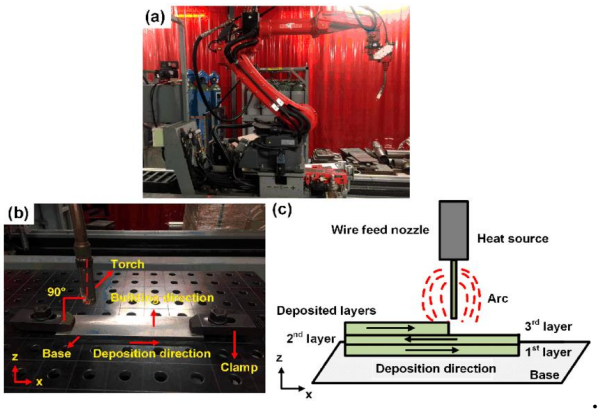

Figure 4. (a) Configuration of robotic WAAM system, (b) setup for experimentation, (c) deposition tool path [54]. Copyright 2019. MDPI, in accordance with CC BY license, Open access.

Genetic Algorithms (GAs) are used how to enhance the parameter selection process in near-net shape deposition for minimizing voids and surplus substances in the WAAM process [54]. An uninterrupted deposition process is planned by verifying overlapping conditions within robot swap zones to avoid collisions [55,56]. Likewise, a continuous deposition process is being planned carefully by checking areas where robots might overlap or come close to each other in robot swap zones. This careful planning is done to prevent any collisions between the robots, ensuring smooth and safe operations. The robotic guidance will be fixed on the desired welding speed which affects the heat accumulation and results in variations of the RS in the products and the robotic guidance to monitor the process in the WAAM described in Figure 4. Employing path planning was proposed [54,55] to incorporate bead overlap and enhance internal structural stability by minimizing height eventually, it influences the RS in WAAM products.

3.2. Residual Stress in WAAMed Products

RS in WAAM refers to the internal stresses that remain locked inside a part (thermal RS) within fabricated components [56]. When a component within this RS is subjected to cyclic loading or stress, it can accelerate the initiation and propagation of the cracks which is the reason for premature failure [57]. This RS may arise from various factors, such as the cycles of heating and cooling associated with the differential expansion during the welding process, contraction of materials during cooling time, and other process parameters [58–63]. Ahsan et al. [64] identified that the high heat input is a near-optimal processing condition to improve surface quality, higher ductility, and higher deposition rate due to the induced high RS. In the WAAM process, the component will induce heat tension and thermal distortion as temperatures fluctuate with the advancement of fabrication [65,66]. This adjustment is made by controlling the values of wire feeding rates and travel speed (TS). With higher heat input the lower RS is observed on the surface of the top layer by long-time cooling durations [67]. Welding RS was measured using five experimental methods: X-ray diffraction (XRD), neutron diffraction (ND), incremental deep hole drilling (iDHD), incremental center hole drilling (iCHD), and contour method (CM) [68].

As researchers delve deeper into WAAM, they have discovered significant enhancements inside the grain arrangement and material properties of the produced components [69]. The transformation of large, elongated grains into smaller, uniformly shaped grains in both the inner and intermediate layers is accomplished by adjusting the amount of heat applied [66,67]. The influence of heat input on the RS, macroscopic structure, microscopic composition, and mechanical characteristics of the components fabricated through the WAAM procedure is studied in [70,71]

3.3. Residual Stress Measurement Methods

Generally, there are two RS measuring techniques, namely experimental and numerical methods, which are reviewed and reported in the following subsections.

 doi:10.20944/preprints202405.0422.v1

3.3.1. Experimental Methods for RS Measurement in WAAM Parts

Several review articles across different literature types have investigated the examination of RS in WAAM products using various techniques [72]. Initially, these studies focused on the stress within central lines, conducting a theoretical analysis of stress evolution along these lines without assuming a specific stress distribution, which is considered RS. Subsequently, the research expanded to improving forecast models for warpage, based on general beam theory[73]. Other techniques encompass neutron diffraction (ND) [22–24,74], X-ray diffraction (XRD) [25–27,75], contour method [13,76–78] hole drilling methods [32], thermomechanical coupling model [79], digital image correlation (DIC) [80], deep hole drilling (DHD) [81], Operando synchrotron or synchrotron X-ray diffraction (SXRD) [82,83]. The selection of the methods depends on elements such as material, component size, geometry, and the level of accuracy required for the measurement. Accurate modeling of the process is crucial for understanding and controlling RS. For instance, XRD analysis is utilized to identify the grain size observed in the thin strips and ferrite of bainite created due to thermal cycles while dye penetration tests are used to investigate surface defects and corrosion behaviors of WAAM components [66,67,84,85].

The choice of the appropriate measurement method is governed by factors such as accessibility, resolution, accuracy, and the desired depth of stress penetration. Table 1 lists the methods used for RS measurement on different materials together with the summary of the experimental studies. As can be observed from the table, the most used methods, according to the literature overview are XRD, ND, digital image correlation (DIC), SXRD, layer removal (deep hole drilling), contour method, and incremental hole-drilling method.

Table 1. Summary of experimental methods for RS measurement.

Methods	Materials	Results	Ref.
ND	316L stainless steel	The process parameters' influence on RS is barely noticeable in the melted zone.	[22]
	Fe3Al alloy	Large columnar grains result in anisotropy and RS is tensile in the building direction, and the tension to compression progressively moves up from the beginning to the end of the deposition way.	[23]
	AA6061	RS indicates the occurrence of tensile stresses with a greater magnitude in the constructed parts, substrate exhibits fewer compressive stresses. No significant dissimilarities were seen in mechanical properties.	[61]
	2319 aluminum alloy	RS along the build direction in the deposited wall is tensile stress, extending up to the floor. The inter-pass rolled walls, reduced RS to enhanced strength in the longitudinal direction.	[24]
	Fe3Al	RS and distortions resulting from the WAAM process are major concerns as they not only influence the part tolerance but can also cause premature failure in the final component during service.	[86]
	stainless steel 304L	The alteration of RS in the specimen after introducing a new deposit. Longitudinal stress was predominantly tensile, reaching its peak at the boundary between the parent material and the layers where the thermal loads were applied.	[87]
	Inconel 625	Measurements showed that lower RS formed in the direct interface functionally graded materials (FGM) compared to the smooth gradient FGM	[88]

 doi:10.20944/preprints202405.0422.v1

Contour and ND	Ti-6Al-4V alloy, stainless steel	The stress in the baseplate varies RS. The lattice parameters were not valid in the baseplate for ND measurements. Cutting out a stress-free exit was used to correct reference samples.	[76,77,89]
XRD	Alloy C-276	The amplitude of tensile RS was perceived in the travel direction compared to the build orientation. The residual strain in the lattice reveals the RS in the material. The larger amplitude of compressive RS was found in the build axis.	[90]
	Al-5356 alloy	The height of the beam can impact both the level and pattern of longitudinal RS in both the substrate and the beam. This variation primarily affects transverse RS in the substrate and has minimal influence on the beam itself.	[91]
	G 79 5 M21 Mn4Ni1.5CrMo (EN ISO 16834-A)	RS, hardness, and microstructure are influenced by welding parameters, geometry, and component design. Heat input causes decreased tensile RS which causes unfavorable grain structure and mechanical response.	[25]
	SS308L austenitic stainless steel (SS)	Accumulation of compressive RS attributed to elevated heat input and rapid cooling rates. Greater stress happened closer to the welding base than in other areas.	[26]
	Al–6Cu–Mn alloy	The advancement of RS indicates that the most crucial area of the sample is near the substrate, where significant tensile stresses near the material's yield strength are dominant.	[27]
	Grade 91 (modified 9Cr–1Mo) -steel	RS varies the characteristics of the material and its microscopic structure WAAMed ferritic/martensitic (FM). The heat treatment applied to the originally manufactured steel did not remove its anisotropic properties.	[83]
	Inconel 625	Post-treatment heat processes can enhance corrosion resistance, and alleviate RS. Measurements indicated that the smooth-gradient approach produced secondary phases like d-phase (Ni3Nb) and carbides, which were absent in the direct interface method.	[88,92]
DIC	Mild steel (AWS ER70S-6)	DIC was employed to oversee the flexural distortion of WAAM components while being released from the clamped H-profiles, and residual tensions were deduced from the strain distribution observed during the unclamping process.	[80,93]
Deep hole drilling	Mild steel (G3Si1) & austenitic SS (SS304)	RSs are under compression in the mild steel section and under tension in the austenitic stainless steel (SS) section. These stresses fluctuate across the thickness because of differences in cooling rates on the interior and exterior surfaces.	[81]
Hole drilling	Ti-6Al-4V	Grain size decreased after ultrasonic impact therapy and RS of fabricated parts in WAAM after post-UIT are improved.	[79,94]
Thermomechanical coupling & Contour	Stainless steels (SS) SUS308LSi	RS is tensile in the layers bordering the surface's upper surface, compressive in the layers near the substrate surface, and tensile near the underside of the substrate.	[13]

 doi:10.20944/preprints202405.0422.v1

The RS measurement techniques listed in Table 1 can generally be classified into three categories: (1) non-destructive; semi-destructive; and (3) destructive are mentioned in Table 1 with short descriptions; while some of the techniques were not performed in the past research. Non-destructive techniques (NDT) like XRD and ND are common high precision and frequently preferred to measure RS in WAAM components. The choice of the methods depends on fundamentals such as material, component size, geometry, and the level of accuracy required for the measurement.

It is clear that from RS measurement techniques, ND has been utilized more extensively by researchers due to its non-destructive nature, which helps maintain the veracity of the parts while X-ray diffraction is the second method utilized. The pie chart shown in Figure 5 represents the hierarchies of techniques used to measure RS in WAAM products.

In principle, the local thermal cycle makes variations of grain structures and finer grain is observed with thin strips of bainite and ferrite which have been confirmed using XRD analysis [84]. Similarly, the elastic strain is calculated from the change of the lattice spacing then RS [23]. In this case, any stress whether external or residual within a material, leads to deformation and changes in lattice spacing. Stress is determined by measuring lattice distance at different tilt angles using Bragg's law, which explains X-ray diffraction in crystal lattice planes. From several NDTs for identifying RS, XRD was mostly selected due to its capability to penetrate approximately 10 μm and provide spatial resolution ranging from 10 μm to 1 mm, rendering it particularly suitable for thin plate applications [26].

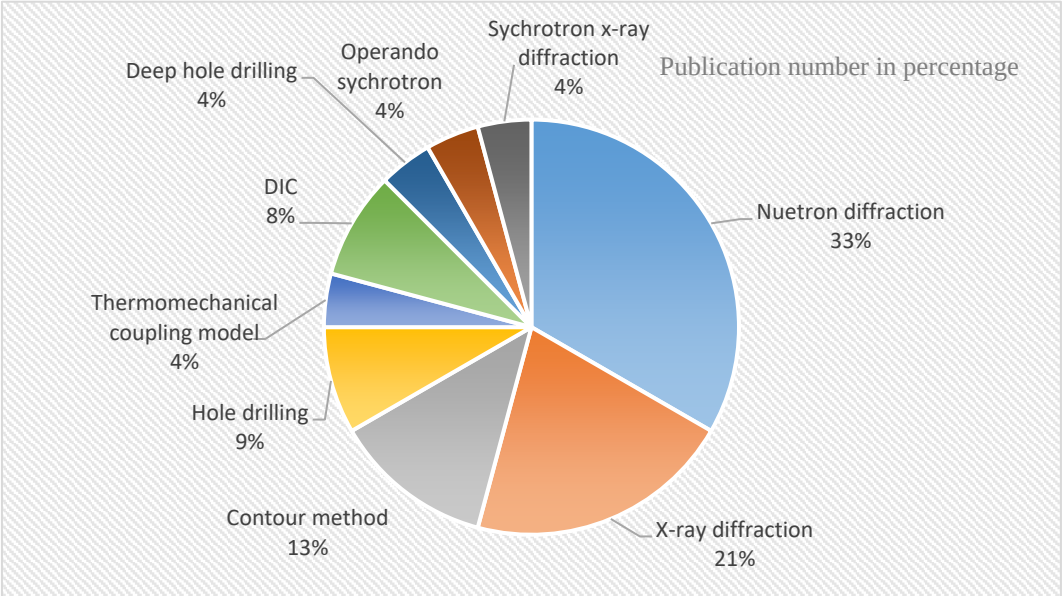

Figure 5. Pie chart research field distribution sorted based on the quantity of RS.

3.3.2. Numerical Analysis of RS in WAAM Products

Basically, behind the numerical analysis of RS, there are mathematical models often based on finite element analysis (FEA) or other computational methods, and the same procedures are performed to determine RS in the WAAM process for simulating thermal and mechanical processes occurring during AM. These models incorporate material properties, process parameters [85], and boundary conditions to simulate the deposition, heat measurements techniques mention the highest proportion and/or the lowest proportion.

Transfer, and subsequent cooling processes. By solving governing equations for heat transfer, numerical simulations predict the evolution of RS within the part. Similarly, the numerical analyses examine how deposition pattern and travel speed affect RS and warpage in WAAM components [95]. Table 2 provides overviews of the numerical analysis techniques, feedstock materials, and their outcomes when utilized in the WAAM process.

 doi:10.20944/preprints202405.0422.v1

Table 2. Overview of reported numerical analysis, tools, and materials related to WAAM technologies.

FEM Softwares	Material	Summary	Ref.
ANSYS	B91 steel (ER90S-B91 steel)	A thermomechanical assessment of WAAM B91 steel was performed sequentially to assess the variation in residual stress throughout the component.	[11]
Simufact	Steels	The dynamic temperature changes, alteration, stress accumulation, and deformation, hold significant importance for applications involving high-strength steels.	[41]
ABAQUS	Aluminum alloy	Deposition pattern and travel speed have an impact on RS and warpage in WAAM parts. Results of thermomechanical FE simulations show that the out-in deposition pattern leads to the highest levels of RS and warpage. Increasing travel speed lowers peak temperature and thermal gradient in deposition, reducing RS.	[95]
	Inconel 718	Utilized a comprehensive 3D transient heat transfer model to calculate the temperature distribution and gradient in the WAAM process for various process parameters which results in RS. The derived temperature data was utilized in a mechanical model to forecast RS and distortion.	[96]
	Carbon steel	The modeling outcomes indicate that as the count of deposited layers rises, the maximum temperature rises resulting in RS while the average cooling rate decreases.	[97]
	Austenitic stainless steel (304) and low Carbon steel (A36)	By systematically altering one mechanical property at a time, we isolated the influence of each on RS formation in dissimilar welds. Results show that longitudinal residual stress in both alike and different welds can be diminished within the weld zone by an amount equivalent to the stress caused by applied mechanical tensile force once the tensioning force is released post-cooling.	[98]
	API X65 steel	Thermal conditions and RS are forecasted precisely to allow for the regulation of the fusion zone's shape, microstructure, and mechanical characteristics in the Submerged Arc Welding joint.	[99]
	Structural steel ER70S-6 wire	The residual stress and deformation of two extensive builds were examined, revealing highly consistent numerical findings and favorable correspondence with experimental outcomes.	[100]
	EH36 steel	The effect of the scanning speed on thermal profiles and RS indicates that higher scan speeds result in reduced peak temperatures and heightened cooling rates, thus leading to a rise in the volume portion of martensite within the deposition.	[101]
	Aluminum alloy	The RS and deformation were computed using the moving heat sources (MHS) method and the segmented temperature function (STF) method.	[102]
	Ti-6Al-4V, S355JR steel & AA2319	Reduced profile radii of roller effectively eliminate almost all tensile RS near the surfaces.	[33]
MSC. Marc	Y309L	Elevated RS is generated within the deposition layers and also within the middle of the substrate.	[103]
	Welding filler G3Si1	Simulation and validation regarding geometry and microstructure variations within the welding passes were conducted with RS reality and simulation using measurement inertia of the thermocouples.	[104]
	S316L	The variances in RS are influenced by both the fluctuating temperature distribution during the freezing phase and the forces applied to the WAAM structure following the cooling process.	[105]
COMSOL-5.4	304 Stainless steel	Large-scale images and high-speed recordings were used for the wall constructed to verify the accuracy of the measurements of the molten pool and the form of the deposition determined which decided the RS in parts.	[106]

Drexler et al. [107] addressed the numerical modeling of RS and distortions occurring in WAAM parts with weaving deposition. Numerically forecasted thermal stresses across various welding

 doi:10.20944/preprints202405.0422.v1

layers were depicted for subsequent experimental evaluation conducted in [108]. Similarly, finite element (FE) simulation along with thermal analysis generated appropriate paths by segmenting a 3D surface scan of the intended repair area [42]. As illustrated in the pie chart in Figure 6 (ref. also Table 2), most of the numerical analysis of RS were investigated using ABUQAS.

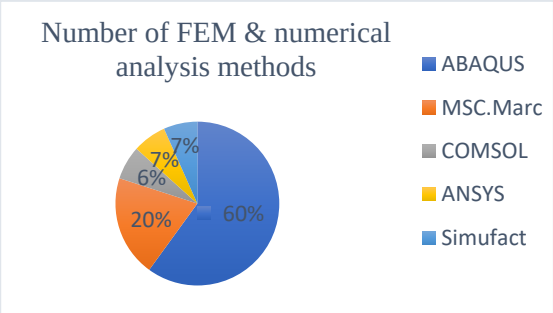

Figure 6. Quantity of publications on FEM used for RS in WAAM process published with some materials.

3.4. Factors Influencing RS in WAAM

Researchers and engineers can characterize and understand the RS behavior in WAAM components by employing experimental methods and Finite Element Analysis (FEA), leading to improved process control, part quality, and product performance. Many parameters that can influence RS in WAAM parts are discussed in [18], while a profile that includes an assessment of the overall height, width, and smoothness of each generated wall was studied and reported in [109]. Deposition parameters [110], heat input,
Interlayer temperature, and the duration of interlayer pauses were significant factors influencing the formation and distribution of pores in aluminum 5183 alloys printed in the WAAM process [111]. Similarly, different welding travel speeds at which defects become noticeable also imply both wire feed speed and travel speed in the welding process [112]. In contrast, substrate (bed or baseplate) thickness was found to have a major influence on the RS distribution along deposit height. Given the substrate, tensile RS as high as the value of the material yield strength was discussed in [113]. The RS distributions in both the longitudinal and transverse directions indicate that longitudinal stress shifts significantly from compression during the deposition to tension in the baseplate [114].

Moreover, a thicker substrate induces greater RS than a thinner substrate. A substrate that is used for molten pool dropped on (printing process) can be made of a 2xxx aluminum alloy plate for aluminum alloy feedstock [115,116]. In the direct 3D printing process, the position of the printed sample matters to the quality of the printed parts [65]. This is because the expansion of isotherms fails to reach the bottom of a thick plate, resulting in increased heat accumulation [117,118]. The technique controlling inherent RS and distortions faces numerous challenges in the WAAM products leading to unpredictable structural integrity in the printed parts. For such reason, some literature identifies that different process parameters like wire feed rate, travel speed, heat input, deposited path length, width, and depth (thickness) of printed components have their effects [47,56,119]. The main defects induced in metal manufacturing components due to these parameters in the WAAM process identified by many investigators are such as RS, deformity, porosity, crack, and distortion. Thus, the most common factors of WAAM products' defects are the process parameters, which limit the acceptance of this technology [120–124]. In another way, undercut and humping are the common defects found in the WAAM products with the major influence of deposition height, width, and stable layer is produced heat input per length values [112].

The processing conditions effects, such as interlayer temperature, deposit height, and substrate thickness on the distribution and magnitude of RS were studied in the literature [113,125,126]. The majority of substrates revealed the rewarding compressive RS while the deposit beads showed tensile stress**.** The instrument of absolute distance measurements is incorporated into the WAAM system to deliver monitoring processes of deposit layer height, profile, and bead volume predictions during

 doi:10.20944/preprints202405.0422.v1

the processes. Micrometers by hand and laser scanning measurements were also used after each completed deposit [127,128]. WAAM encompasses a multitude of adjustable process parameters, such as wire feed rate, voltage, current, travel speed, and layer height [129]. These parameters govern various aspects of the deposition process, including heat input, cooling rate, and thermal gradients. Understanding how alterations in these parameters influence RS is vital for achieving optimal WAAM products' performances [112]. Selection of bead geometry parameters in the WAAM process is required to optimize excess materials and minimize the void created in the multiple layers of bead depositions. Process Parameters and other factors influencing RS in WAAM components are summarized and listed in Table 3.

Table 3. Factors influencing RS in the wire arc additive manufacturing.

Process parameters and other factors	**Short description**	**Ref.**
Material properties: *weldability of the materials*	Not all materials are equally suitable for WAAM. The process often requires materials with good weldability characteristics, such as low susceptibility to cracking and good fusion properties. For instance, materials' thermal conductivity, coefficient of thermal expansion, and phase transformations can impact RS induced.	[13,35,130,131]
Deposition power: *Arc current & voltage*	In the WAAM process controlling the heat input is critical to prevent overheating, distortion, and metallurgical issues such as excessive grain growth or phase transformations. Variations in heat input alter materials' weldability consequences of RS.	[25,66,67,115,132,133]
Speed: *wire feed speed, welding travel speed, and deposition rate*	Rapid deposition and cooling can lead to increased RS, especially near the deposition zone. The rapid solidification and higher deposition rate can cause thermal gradients and differential cooling rates, resulting in higher levels of tensile RS. Increasing the welding travel speed reduces the amount of time the material spends in the high-temperature zone and leads to lowering the magnitude of RS.	[112,134–136]
Shielding gas: *types of shielding gas, and shielding gas flow rate*	Shielding gas plays a crucial role in WAAM processes as it protects the molten weld pool from atmospheric contamination and influences the heat transfer characteristics during deposition. Both the type of shielding gas, gas flow rates such as argon and helium, and reactive gases like CO_2 and O_2 can have significant effects on RS formation in WAAM products.	[3,38,137]
Nozzle distance: *Nozzle tip to work distance (Welding torch distances*)	The welding torch distance, in WAAM processes can have a significant influence on RS in the final products. Optimizing the nozzle tip to work distance in WAAM processes involves balancing the heat input, cooling rates, distortion control, interlayer bonding, and defect formation to minimize RS and ensure the production of high-quality parts.	[23,24]
Printing position: *Electrode to layer angle (wire) (θ) and layer height*	The printing position affects heat dissipation and buildup, influencing the cooling rate and thermal gradients within the part. The printing position affects the flow of molten metal and the geometry of the deposited beads results in variation of RS.	[37,65,130,138,139]
Layer thickness: *Substrate thickness, deposition thickness*	Decreasing the layer thickness in WAAM fabrication can lead to shorter thermal cycles and reduced heat input per layer. This may result in lower overall RS due to less thermal distortion and reduced HAZ size.	[126,140]
Cooling rate: *Deposition of layer time, dwell time between layers*	The rapid heating and cooling cycles involved in WAAM can lead to the development of significant RS and distortion in the fabricated parts. These can adversely affect the structural integrity and dimensional accuracy of the components, making it challenging to achieve desired weld properties and, as a result, change the RS in printed parts.	[58–61,103,141]
Preheating substrate (Baseplate)	Preheating the substrate in WAAM processes offers several benefits for managing RS in the final products. By reducing thermal gradients, mitigating distortion, improving metallurgical	[97,142,143]

 doi:10.20944/preprints202405.0422.v1

	bonding, enhancing ductility, and optimizing cooling rates, preheating helps to create parts with lower levels of RS and improved mechanical properties.	
Part geometry: *Printed part shapes & volume of the parts*	The geometry of printed parts in WAAM processes significantly influences RS. Understanding how shape complexity, part orientation, volume, and material accumulation patterns affect thermal gradients and cooling rates is crucial for managing RS and ensuring the production of high-quality parts with desired mechanical properties and dimensional accuracy in WAAM.	[9,26]
Post-Weld Heat Treatment (PWHT)	PWHT plays a crucial role in managing RS in WAAM products. By subjecting the parts to controlled heating and cooling cycles, PWHT can effectively alleviate RS, improve material properties, and enhance the overall quality and implementation of the manufactured parts.	[1,4,61,117,144]
Scanning pattern	The scanning pattern plays a crucial role in influencing heat accumulation, cooling rates during AM deposition, and consequently, the formation of RS.	[101]
Wire filler: *wire filler diameters and wire grade*	The filler wire diameter and wire grade are two key factors that can significantly influence RS in WAAM products.	Not studied

The height of the bead, width, and cross-sectional area of the beads are expressed using the process parameters [145]. Furthermore, the diameter of the wire is expected to significantly influence both the melting efficiency of the wire and the mode of metal transfer, which are crucial factors in enhancing the deposition rate of WAAM. Nonetheless, the comprehensive effects of wire size on process attributes and deposition rate in plasma transfer arc-based WAAM remain inadequately comprehended. The primary objective is to examine the optimal combination of wire diameter with the Wire Feed Speed (WFS) to achieve higher deposition rates and improved bead geometry, while also addressing process control challenges and defect avoidance at elevated deposition rates. All aspects of limitation of deposition rate, bead shape control, keyhole formation, and metal transfer are studied in [43]. The selection of welding parameters in the WAAM is investigated in [146] and the values of the range used are explained in [147]**.** In the pie chart diagram in Figure 7, the factors that influence the residual stress in WAAM parts are plotted in percentages.

The elevation of the bead grows in a nearly proportional manner with the rise in wire feed rate, while the width of the bead decreases only at the subsequent feed rate. Moving on to the travel speed, it's observed that the width of the bead diminishes as the travel speed increases, whereas the bead height remains relatively constant. Furthermore, the wetting angle decreases as the travel speed increases [148]. The explanation of computing heat input per unit volume is outlined. The research indicated inconsistencies among various standards in interpreting heat input. Furthermore, the practical implementation of the method for calculating the precise heat input into the weld was validated [132]. Naveen et al. [149] conducted research by focusing on process parameters effects on product made of 5356 aluminum alloy on WAAM with three parameters namely; (1) wire feed rate, (2) welding speed, and (3) gas flow rate of value product of weld beads. The technique adopted was the Taguchi method to decrease the trial number for choosing a range of input variables. Successful efforts have been made to optimize welding modes for the WAAM applications in which more grain microstructure is studied [150].

 doi:10.20944/preprints202405.0422.v1

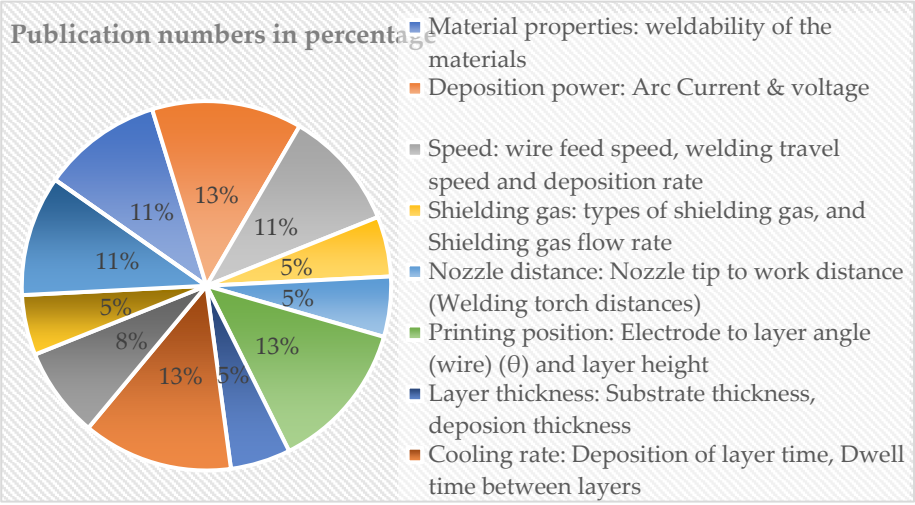

Figure 7. Pie chart of research field distribution sorted based on the number of factors influencing RS.

The Taguchi technique along with ANOVA was employed to analyze how travel speed, wire feed rate, current, and argon flow rate impact various outcomes such as bead shape and size, bead roughness, oxidation levels, melt-through depth, and microstructural characteristics [148]. Based on the energy dissipation hypothesis and associated equations, various additive manufacturing processes utilizing energy beams can be compared more thoroughly when subjected to equal energy input. This comparison serves as a foundation for determining the initial process parameters and the dynamic adjustment of main parameters [151]. The amount of heat input generated in the welding arc per unit length of the weld is expressed in kilo Joules per millimeter length of the weld (kJ/mm) as shown in Eq. (1).

$$\text{Arc energy (kJ/mm)} = \text{Volts x Amps } = V \times I \tag{1}$$

where V is in volts, and I is in ampere (A). The amount of heat input generated in the welding arc per unit length of the welding process is represented as in Eq. (2) and in different ways as per the ASME IX QW-409.1 standard from the American Society of Mechanical Engineers [132].

$$\text{Heat Input (J/mm)} = \frac{\text{Volt}\times\text{Amps}\times 60}{\text{Travel Speed}(mm/min)} = \frac{\text{V}\times\text{A}}{\text{v}} \tag{2}$$

where v is the travel speed. Vora et al. [152] investigated that voltage had the greatest influence on bead width, followed by travel speed and the ratio of gas mixture.

The deposited layer during the fabrication process for bead formation is assumed to be semi-circular. The deposition rate, R, which is influenced by wire diameter, wire feed speed, and wire density is expressed as Eq. (3).

$$\text{R} = \frac{\pi \text{d}^2 \text{v} \rho}{4} = \rho \text{v} \text{A}_{\text{ww}} \tag{3}$$

where d is the wire diameter, v, is the wire feed speed (WFS), ρ is the wire density and welding wire cross-section area.

4. Impact of RS on Mechanical Properties in WAAM Components

Although WAAM has shown its capability to produce medium-to-large-sized components from aluminum for automotive and related industries, it cannot yet serve as a comprehensive production method due to practical challenges such as unmatched mechanical properties and significant RS [153]. RS significantly affects the materials and mechanical characteristics of the manufactured component. For instance, it can affect the mechanical properties, such as strength, hardness, and ductility of products, by making them different from the material's intrinsic properties. High heat supply in the WAAM process results in reduced tensile stress within the component and can lead to undesirable mechanical properties and microstructure [154,155].

 doi:10.20944/preprints202405.0422.v1

Microstructural characteristics have an impact on the material properties of parts. Due to the existence of RS in WAAM products caused by the rise in either welding speed or the heat distribution parameter, material properties can be significantly varied [108,156]. The resultant microstructure and RS level in WAAM are directly correlated with the ultimate mechanical properties. Extensive research has been conducted on WAAM due to significant internal porosity in beads formed and its capability to produce large-scale components demonstrates inadequate tensile and fatigue properties [157]. This porosity is a result of RS by affecting the solidification process and the ability of gas to escape during deposition [158,159]. Similarly, RS can influence various mechanical properties of the manufactured parts in several ways by changing strength, toughness, microstructure, fatigue life, cracking, and delamination of the WAAM products [160]. RS formed during the fabrication process markedly impacts mechanical performance and may result in detachment from support structures, undesired shape deformation, and premature crack initiation [77]. The input parameters, resultant microstructure, post-manufacturing treatments, and RS have significant impacts on the ultimate mechanical characteristics of WAAM products [1,161,162]. The accuracy of the formation of the deposition layer is influenced not only by the precision of the arc torch's positioning but also by the stability of the forming process [163].

Figure 3 depicts the challenges and inherent RS in WAAM parts where reheated and re-melted parts are the known phenomena in high technology during the manufacturing process. To achieve good grain structure in each layer, the minimum penetration depth of plastic strain should exceed the sum of the re-melting depth and the height of the newly deposited layer. To enhance the microstructure, the minimum depth of plastic strain must exceed the combined depth of re-melting and the height of the newly deposited layer [33].

The experiments for the investigation of RS were conducted on the WAAM-based products by using cladding of single beads using welding voltage and current parameters as variables. The dependence of the formation of beads on the number of short circuits per unit length is explained in [50]. Even though the WAAM technology is an energy-efficient manufacturing method for metal production, heat accumulations during deposition, metallurgical, and associated mechanical properties results can change the RS profiles across the cross-section of the fabricated components [11,13,164]. The impact of build orientation and heat treatment schedule on the microstructure and mechanical properties of thin-walled components was examined in [165]. The distributions of RS within the component along the deposition path, both internally and externally are equal to zero [166,167].

Overall, understanding and controlling RS are essential for ensuring the mechanical reliability, dimensional accuracy, and functional performance of WAAM products in various applications. Many research efforts focused on characterizing RS, developing predictive models, and implementing advanced manufacturing techniques, which are critical for advancing the field of WAAM and unlocking its full potential in industrial applications [103]. Comprehending the distribution of heat input and its implications, including transient temperature distribution, material transformation, stress accumulation, and distortion, holds significant relevance for applications involving high-strength steels. Numerical simulation can offer valuable insights for assessing these factors [41].

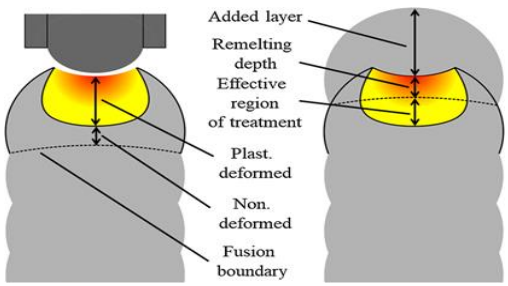

Figure 8. Diagram illustrating the re-melting phenomenon occurring during the deposition process [33] . Copyright 2019, in accordance with CC BY license, Open access.

 doi:10.20944/preprints202405.0422.v1

The RS and deformation significantly impact the performance of the components [102]. As a result of repetitive cycles, RS becomes confined within the components, causing an array of defects such as cracks, deformations, warping, and diminished component lifespan [168].

5. Mitigation Strategies for RS in WAAM and Practical Applications

The generation of RS and distortion in parts impedes its broad adoption due to the intricate thermal build-up histories characteristic of WAAM components [169]. However, mitigation strategies for RS in various manufacturing processes in WAAM, involve several techniques to reduce or manage the RS that can impact the reliability and functionality of manufactured components. A hybrid process of WAAM and high-pressure rolling able to build large-scale components produces low detrimental RS and distortion [170,171]. In the same way, numerical methods can offer an additional understanding of how rolling can be effectively utilized to diminish RS and generate the necessary plastic strains to enhance microstructural properties [33]. Combining the WAAM process with other fabrication processes, including machining or subtractive techniques, can assist in removing excess material. This hybrid manufacturing is used in the medical device industry to produce low-stress WAAM parts with complex geometries or add complementary features to reduce RS [172].

Controlling RS is vital for ensuring the durability and reliability of these critical components [135]. A compilation of different methods for mitigating RS and distortion in WAAM has been assembled to offer a blueprint for future advancements [173]. Finite element process simulation offers an effective method to explore strategies to mitigate these distortions and RS [174]. Some methods provided techniques to handle RS, enhance mechanical properties, and eliminate defects like porosity [31,175]. Some common mitigation strategies and practical applications are listed and explained with practical application in Table 4.

Table 4. Mitigation strategies for RS and practical applications.

Methods	Material and Strategies	Practical Applications And Results	Ref.
Inter pass rolling	Ti-6Al-4V alloy	Enhances the bonding and adhesion between the successive layers of material. It also helps redistribute stresses by applying compressive force leading to refined grain structures and minimizing distortion results minimize RS.	[24,76,77,176]
Heat treatment (HT)	Grade 91 steel, Ti-6Al-4V	HT post-processing involves controlled heating and cooling cycles to relieve RS. HT is extensively utilized within the aerospace sector to reduce RS in WAAM to produce turbine blades, improving fatigue life and performance.	[83,144,177]
Shot peening	2319 aluminum alloy	Shot peening entails subjecting the surface of a component to bombardment with small, high-velocity particles to induce compressive stresses that counteract tensile RS. It is employed in the automotive sector to enhance the fatigue resistance of WAAM-produced suspension components.	[178,179]
Rolling and laser shock peening	Low carbon steel	The methods eliminate harmful tensile RS at the top of the WAAM wall, thereby enhancing fatigue life and slowing down crack growth rates. The bottom region of the WAAM wall demonstrates improved RS conditions, leading to enhanced fatigue performance, all achieved without surface rolling treatment.	[180]
Rolling	AA2319, S335JR steel	Increased rolling loads result in elevated maximum equivalent plastic strain and deeper penetration of the equivalent plastic strain results in RS.	[33]
Parameter optimization	Al-Cu4.3-Mg1.5 alloy	Adjusting WAAM process parameters, such as deposition speed and layer thickness, can optimize the build conditions to diminish RS. Systematic parameter optimization is applied in the construction industry to reduce RS in large-scale WAAM-printed metal structures.	[37]
Material selection	aluminum alloys	Choosing materials with tailored properties, such as low thermal expansion coefficients, can minimize RS formation during WAAM.	[181,182]

 doi:10.20944/preprints202405.0422.v1

		Specialized materials are used in the energy sector to create high-performance WAAM components with reduced RS.	
In-process monitoring and control	IN718 Superalloy	Real-time monitoring and control systems adjust process parameters during WAAM to minimize RS formation. In-process monitoring and control are used in aerospace manufacturing to reduce RS variations in critical engine components.	[183]
Hot-rolling and cold-forming	ER70S-6 welding wire	The incorporation of WAAM stiffeners at the flange tips of hot-rolled I-sections is demonstrated to result in the creation of favorable tensile RS, which are beneficial for structural stability, reaching maximum values equivalent to the material's yield strength.	[184]
Peening and UITs	Ti alloy & Al alloy	Through Ultrasonic Impact Treatment (UIT), grain refinement and randomization of orientation are accomplished, contributing to the enhancement of RS and mechanical strength.	[185]
Rolling	Titanium alloys	Offer substantial advantages such as diminishing RS and distortion, as well as refining grain structure.	[186]

In this study, we explore how various factors such as process parameters, substrate heating, and cooling influence bead appearance formed during WAAM of Inconel 625 on EN 8 steel. Additionally, the track of temperature history of the molten pool during deposition using an IR pyrometer and examine how these factors affect the cooling rate, which in turn impacts the bead geometry [142,187]. For the morphological aspect of the beads, it is essential to respect the volume of material supplied and the size of the part [188]. The graphs in Figure 8 illustrate the distribution of published work on approaches used to mitigate residual stress and indicate the frequency of their adoption in WAAM applications. This graphs present different mitigation methods of RS in WAAM process versus the utilized number of methods published in articles.

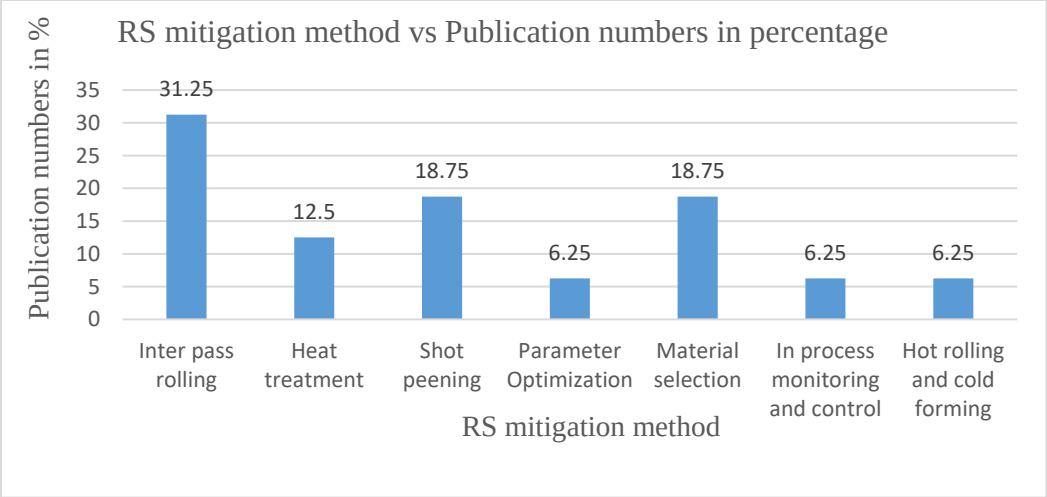

Figure 8. Mitigation method of RS vs publication in percentage.

The graph illustrates the hierarchy of various RS mitigation techniques on successively deposited layers, while other methods are the treatments after production is finished. For instance, inter-pass rolling is mostly applied during the printing process to refine the grain structure, bonding, and adhesion between the consecutive layers of deposit materials. Heat treatment and shot peening are used after fabrication is completed, whereas, process monitoring and control are the mitigation methods used during the printing process.

An approach was developed to analyze the shape of the constructed wall, focusing on its inherent symmetry to ensure efficient material utilization. Additionally, it employs thermography techniques to monitor the symmetry of the melting pool [18]. This volume deposition geometry V (m^3) can easily be deduced from the path (more specifically the travel length of the welding path l_{scan} (m)), the speed of the wire v_w (m s^{-1}), the diameter of the wire d_w (m), and the welding speed v_t (m s^{-1}) [26,148] as expressed in Eq.(4).

Preprints.org (www.preprints.org) | NOT PEER-REVIEWED | Posted: 8 May 2024 doi:10.20944/preprints202405.0422.v1

$$V = \pi d_w^2 \times v_w \times \frac{l_{scan}}{v_t} \tag{4}$$

For a given bead width (w), layer thickness (h), and penetration depth (p) of the bead from the molten pool during the WAAM process, the shape of the bead shape is shown in Figure 9. These parameters are important because wider beads offer improved material coverage, leading to a smoother surface finish, while maintaining a controlled bead height minimizes surface irregularities for a smoother finish. Therefore, modeling of the bead profile is required to establish the relationship among different process parameters. Some studies consider the shapes of beads formed in WAAM process as ellipses [189,190]. The WAAM process constructs intricate parts by layering weld beads, it's vital to model both individual weld beads and the overlapping of multiple beads to ensure superior surface quality and dimensional precision in the fabricated parts. This begins by developing models for single weld beads using diverse curve fitting techniques [191,192].

The geometric representation of different overlapping beads, combined with an algorithm, determines the process conditions required for both materials to achieve consistent bead layer heights [193]. A geometrically flawed segment of a bead, or geometric defect, is a flaw resulting in voids within the final printed part because of incomplete fusion between two irregularly shaped overlapping bead segments [194]. It is preferable to write the same parabola in terms of the process parameters v_w, wire feed speed, and v_t- torch speed. The geometric configuration of the weld bead created through WAAM differs from that of conventional welding methods [195,196]. The bead profile on the substrate can be considered as a symmetric parabola shape which is given in Figure 9 is presented in Eq. (5).

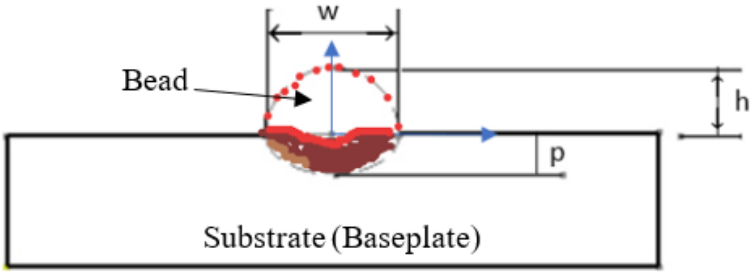

Figure 9. Bead formation of the parabolic profile during the WAAM process.

$$y = a + cx^2 \tag{5}$$

To solve for a and c in Eq (5), the thickness (height) and width of the beads is substituted into the parabola equation to find the constants *a* and *c*. The turning points or vertex is at (0, *a*) for this form of the equation. The parabola is concave downwards because the result of $c < 0$ as depicted in Figure 9 and the bead profile expressed as parabolic eqaution can be solved as Eq. (6).

$$a = h; \qquad c = -\frac{4h}{w^2}$$

$$y = h\left[1 - \left(\frac{2hx}{w}\right)^2\right] \tag{6}$$

The area of a bead (area of the parabolic bead) relative to its geometric parametric is obtained from Eq. (7).

$$A = \frac{2hw}{3} \tag{7}$$

The volume flow rate is expressed in Eq. (8),

$$Q = \frac{2}{3} hw \times v_t \tag{8}$$

 doi:10.20944/preprints202405.0422.v1

For the wire, when the molten pool flows, the volume flow rate is given by Eq. (9).

$$Q = \frac{\pi}{4} d_w^2 \times v_w \tag{9}$$

where d_w is the wire diameter and v_w is the speed of the wire. Equating Eqs (8) and (9), the width-w of the bead is determined from Eq. (10).

$$w = \frac{3\pi d_w^2 v_w}{8 h v_t} \tag{10}$$

From Eq. (10), replacing for w in the Eq. (6) will give Equation (11).

$$y = h\left[1 - \left(\frac{16 h v_t x}{3\pi v_w d_w^2}\right)^2\right] \tag{11}$$

For the different wire diameters, the beads formed vary in thickness and width. However, the shape of the deposited bead is greatly influenced by many welding parameters, including torch angle, wire travel speed, filler feed rate, and cooling conditions [197]. For a given layer thickness (h), bead width (w), and torch speed (v_t), the volumetric flow rate (Q) required for complete filling is given by Eq. (12).

$$Q = v_t w h \tag{12}$$

Setting optimum parametric in the WAAM process would be advantageous for the gradual deposition of weld beads layer by layer in the AM of components [198,199]. Koli et al. [133] studied the WAAM products made of wire of SS308L with a 1.2 mm diameter used to manufacture the samples. The parameters such as welding speed, arc current, and shielding gas flow rate were the most influential in affecting the multiple responses of WAAM products.

The practical applications of components printed by WAAM processes are mainly applicable in the automotive [160], aerospace[200], naval, and defense [201,202] industries' using materials like aluminum due to their high quality and strength with less mass. Generally, WAAM is highly demanded across industries such as automotive, aerospace, chemical plants, maritime, nuclear, shipbuilding, and energy, where it is utilized for fabricating components like aircraft parts, automotive chassis, and marine propellers [8,65,208,209,88,153,156,203–207]. The WAAM process in these industries widely used aluminum alloy series such as 2xxx (Al-Cu), 4xxx (Al-Si), and 5xxx (Al-Mg) [204,210,211]. Aerospace components produced in the WAAM process such as turbine blades, airfoils, and structural elements, need to be carefully controlled RS to prevent premature failure and maintain high-performance standards [86,135,212,213]. WAAM is also used for producing engine parts like cylinder heads and pistons [135].

6. Discussion

Besides the measurement of RS mentioned earlier, certain welding-related defects may potentially occur in WAAMed components. These measurements include many factors that influence the magnitudes of the RS WAAM which are described in Table 1 with several references. The inclusions primarily consist of three classifications of RS measuring methods which are discussed in Section 3.4. From these three, non-destructive measuring techniques are mostly applicable. However, in large samples, the strain of certain components may be difficult to determine or cannot be precisely identified due to variations of dissimilar RS in the penetration depth beam light through the components [214]. Still further research is required to thoroughly examine the RS present in WAAM products resulting from different process parameters. Post-fabrication heat treatment processes can significantly impact the elimination of defects. Though many defects could be eliminated in

 doi:10.20944/preprints202405.0422.v1

WAAMed products, RS was only minimized to the greatest extent possible through heat treatment [136] and other processes mentioned in Table 4.

The quality of metal components fabricated in WAAM relies seriously on key parameters such as travel speed, heat input, wire feed rate, deposition direction, material properties, etc., and others are mentioned in Table 1. While high heat input is necessary to achieve a rapid deposition rate in WAAM, it also presents challenges like RS and distortions. Therefore, managing heat input becomes crucial, especially when fabricating large metal components using WAAM, as it directly impacts both deposition rate and structural integrity [1,47].

6.1. Challenges and Limitations

Like any manufacturing technique, WAAM comes with its own set of challenges and limitations in the measurement and control of RS. It can be used to fabricate complex geometries which makes it difficult to predict and measure RS accurately, especially in intricate structures. WAAM products often exhibit heterogeneous microstructures and material properties due to the fast solidification and thermal cycles experienced during deposition. The variations such as material composition, grain structure, and phase transformations can influence the magnitude and distribution of RS, complicating measurement and interpretation. Measuring RS in the products of WAAM poses several challenges due to the unique characteristics of the process of manufacturing and the resulting material properties. For example, non-destructive testing techniques such as ultrasonic testing or X-ray diffraction are promising for measuring RS in WAAM products, adapting these techniques to the unique characteristics of additive manufacturing materials and geometries presents technical challenges. The common challenge during the test is the capacity of beam light penetration depth dimensions through the printed products. WAAM involves the successive deposition of layers of material, which can result in anisotropic RS distributions. Measuring and characterizing these complex stress patterns accurately requires advanced techniques capable of analyzing stress variations in different directions and depths within the material [215].

The properties and behavior of different materials can vary significantly in different manners and make it challenging to establish a universal approach for RS measurement and control. Management of RS is a critical aspect in the WAAM to ensure the quality and performance of the manufactured components. There were limited industry standards for measuring and controlling RS in the WAAM. The absence of standardized procedures can hinder the adoption of this technology in critical applications. Many investigations can't give a specific magnitude of RS, rather they indicate numerical results and show the character throughout the fabrication operations of WAAM by modeling.

Quantifying this RS is not assigned for all process and welding parameters. For instance, from the input parameters like wire diameter, art welding directions, length, width, thickness, and volume of the products there is a comparison of the printed components. Likewise, from parameters related to welding, such as speed of welding, welding gas, gas flow rate, volts, peak currents, and shielding gas [1,4]. The techniques used in the past investigations for measuring RS in the WAAMed products are already listed in Table 2.

In the other case, shielding gas, types of shielding gas, and its flow rate affect the distribution and amount of RS in products of WAAM. Similarly, the shielding gases types with their flow rate such as argon and helium, and reactive gases like carbon dioxide and oxygen can have significant impacts on RS formation in WAAM products [3,137,148]. However, researchers didn't identify the optimum amount of the shielding gas and types of shielding gas with other processes and input parameters during the WAAM process. Additionally, several reasons that make RS in WAAM are rapid heating and cooling, multi-layer deposition, process parameters, material phase transformations, and part geometry.

The literature review, in general indicates that continuous investigation and improvement in these areas are essential for advancing the understanding and control of RS within WAAM product applications.

 doi:10.20944/preprints202405.0422.v1

6.2. Future Directions

Challenges and limitations for controlling RS in products of WAAM are discussed in Section 6.1. Based on the measurements, mitigations, and limitations found in the past research, which can be mentioned and recommended more studies in future investigations could focus on optimizing the parameters of the WAAM process. By elucidating the intricate relationship between process parameters in WAAM and RS, this review contributes and leads to optimizing the process of parameters, using RS measurement techniques and the assurance of product reliability [85] Likewise, some of the RS measuring methods which are not been performed yet in the products of WAAM in the past research are:

(1) Non-destructive metho
- Ultrasonic Waves
- Magnetic Barkhausen

(2) Semi-destructive methods
- Ring Core
- Deep Hole method

(3) Destructive methods
- Bridge Curvature
- Sectioning Techniques
- Slitting or Crack Compliance

In another way, the filler wire diameter directly affects the deposition rate and heat generated in WAAM. Larger wire diameters typically result in higher deposition rates but also lead to increased thermal input rate per unit length. This increased heat input can influence the cooling gradients and heat input gradients within the deposited material, affecting the spread and extent of RS. The influence of wire diameter over the molten pool deposition to form beads is described in Section 6 using formulas to present the relationships between height and width throughout the WAAM process. For the significant impact of wire size, the optimum size of wire diameters on the RS in the products of WAAM has not been identified in past investigations. Also, among the categories of measuring RS, the appropriate techniques and limitations with formed-bead geometry are not studied.

Since the past researches are not inclusive regarding materials dependence, methodology modifications, application area, and related research issues of WAAM in existing literature, there is ample opportunity for upcoming research to explore various possibilities, including:

1. Most researchers used frequently non-destructive methods like XRd, ND, and some other semi-destructive and fully destructive techniques of measuring RS in components' WAAM. Thus, future studies can perform those techniques listed above.
2. In the future, researchers should determine the most suitable quantity and varieties of shielding gas, in addition to other process and input parameters, throughout the WAAM processes.
3. As explained in Section 5, the mathematical formula provides a particular formation of bead profile and the relationship of wire diameter with the width and thickness (height) of beads. The result of variation in wire diameter, the thickness, and width of beads can vary consequently heat distribution of the process results in a variation of RS in WAAM parts. Therefore, the future researcher can focus on a variety of wire diameters to reduce RS in WAAM parts with less diameter of wire diameter.
4. Materials weld-ability depends on their physical properties that influence the accumulation of RS in products of WAAM. In the future, further research endeavors should aim to investigate these physical properties of materials which are listed in Table 3, and other robot adjustable effects to RS fabricated components through WAAM.

7. Conclusions

In conclusion, this literature review has delved deeply into the extensive research surrounding the investigation and measurement of RS in WAAM products, with specific emphasis on the influence of fabrication parameters. The significance of RS in determining the material characteristics

 doi:10.20944/preprints202405.0422.v1

and structural integrity of WAAM components has been underscored throughout the review work. Moreover, the study has provided an all-inclusive summary of key findings, measurement methods, problems, and future directions in the WAAM dynamic field.

The review highlights the critical role of RS in shaping the dimensional constancy of WAAM products, emphasizing the necessity of precise measurement and control for effective utilization. Synthesizing diverse research studies, techniques, and methodologies, the review work has offered a valuable understanding of the present research status in this domain. Furthermore, this review serves as a guide for future researchers to use the other RS measurement techniques those that have not been performed yet and compare previous techniques used in the literature. To measure RS WAAMed products, experimental methods including semi-destructive (only hole-drilling), destructive (contour method), and non-destructive techniques (such as neutron crystallography and X-ray diffraction, digital image correlation, and Synchrotron X-ray diffraction) have been reported through literature.

Overall, this review is inclusive of examining and measuring RS techniques in WAAM products based on input parameters and other influences of RS products. Through meticulous evaluation and coordination of existing literature, this review underscores the importance of understanding the factors influencing and mitigation methods of RS in products of WAAM.

Author Contributions: The roles of the authors in this study are outlined as follows: F.D.G. came up with the title and contributed to conceptualization, methodology, investigation, and original draft preparation. H.G.L. contributed to the conceptualization and provided resources, supervision, project administration, editing, reviewing the manuscript, and securing funding. Y.W.A. participated in editing and reviewing the manuscript. M.D.H. has also participated in organizing and data analysis in the manuscript. All authors have reviewed and approved the final version for publication.

Funding: This study received backing from the INDMET initiative under grant number 62862, which was financed through the NORHED II program.

Institutional Review Board Statement: Not applicable.

Informed Consent Statement: Not applicable.

Data Availability Statement: Not available.

Conflicts of Interest: The authors declare no conflict of interest.

References

1. Bhuvanesh Kumar M, Sathiya P, Senthil SM. A critical review of wire arc additive manufacturing of nickel-based alloys: principles, process parameters, microstructure, mechanical properties, heat treatment effects, and defects. J Brazilian Soc Mech Sci Eng. 2023; Volume 45, pp. 1–27.
2. Tangestani R, Farrahi GH, Shishegar M, Aghchehkandi BP, Ganguly S, Mehmanparast A. Effects of Vertical and Pinch Rolling on Residual Stress Distributions in Wire and Arc Additively Manufactured Components. J Mater Eng Perform. 2020; Volume 29, pp. 2073–84.
3. Derekar KS. Aspects of wire arc additive manufacturing (WAAM) of alumnium alloy 5183. Award Inst Coventry Univ. 2020; pp. 1–227.
4. Rodrigues TA, Duarte V, Miranda RM, Santos TG, Oliveira JP. Current status and perspectives on wire and arc additive manufacturing (WAAM). Materials. 2019; Volume 12, pp. 1121.
5. Laghi V, Palermo M, Gasparini G, Veljkovic M, Trombetti T. Assessment of design mechanical parameters and partial safety factors for Wire-and-Arc Additive Manufactured stainless steel. Eng Struct. 2020; Volume 225, pp. 111314.
6. Cunningham CR, Flynn JM, Shokrani A, Dhokia V, Newman ST. Invited review article: Strategies and processes for high quality wire arc additive manufacturing. Addit Manuf. 2018; Volume 22, pp. 672–86.
7. Klobčar D, Baloš S, Bašić M, Djurić A, Lindič M, Ščetinec A. WAAM and Other Unconventional Metal Additive Manufacturing Technologies. Adv Technol Mater. 2020; Volume 45, pp. 1–9.
8. Mathews R, Karandikar J, Tyler C, Smith S. Residual stress accumulation in large-scale Ti-6Al-4V wire-arc additive manufacturing. Procedia CIRP. 2024; Volume 121, pp. 180–5.
9. Wu B, Pan Z, van Duin S, Li H. Thermal Behavior in Wire Arc Additive Manufacturing: Characteristics, Effects and Control. Transactions on Intelligent Welding Manufacturing. Springer Singapore; 2019; pp. 3–18.

10. Williams SW, Martina F, Addison AC, Ding J, Pardal G, Colegrove P. Wire + Arc additive manufacturing. Vol. 32, Materials Science and Technology (United Kingdom). 2016; pp. 641–647.
11. Jimenez X, Dong W, Paul S, Klecka MA, To AC. Residual Stress Modeling with Phase Transformation for Wire Arc Additive Manufacturing of B91 Steel. Jom. 2020; Volume 72, pp. 4178–86.
12. Jin W, Zhang C, Jin S, Tian Y, Wellmann D, Liu W. Wire arc additive manufacturing of stainless steels: A review. Appl Sci. 2020; Volume 10, pp. 1563.
13. Huang W, Wang Q, Ma N, Kitano H. Distribution characteristics of residual stresses in typical wall and pipe components built by wire arc additive manufacturing. J Manuf Process. 2022; Volume 82, pp. 434–47.
14. Mohan Kumar S, Rajesh Kannan A, Pravin Kumar N, Pramod R, Siva Shanmugam N, Vishnu AS, et al. Microstructural Features and Mechanical Integrity of Wire Arc Additive Manufactured SS321/Inconel 625 Functionally Gradient Material. J Mater Eng Perform. 2021; Volume 30, pp. 5692–703.
15. Kumar V, Singh A, Bishwakarma H, Mandal A. Simulation of Metallic Wire-Arc Additive Manufacturing (Waam) Process Using Simufact Welding Software. J Manuf Eng. 2023; Vlume 18, pp. 080–5.
16. Knezović N, Topić A. Wire and Arc Additive Manufacturing (WAAM) – A New Advance in Manufacturing ., Lecture Notes in Networks and Systems. Springer International Publishing; 2019; Volume 42, pp. 65–71.
17. Costello SCA, Cunningham CR, Xu F, Shokrani A, Dhokia V, Newman ST. The state-of-the-art of wire arc directed energy deposition (WA-DED) as an additive manufacturing process for large metallic component manufacture. Int J Comput Integr Manuf. 2023; Vlume 36, pp. 469–510.
18. Barath Kumar MD, Manikandan M. Assessment of Process, Parameters, Residual Stress Mitigation, Post Treatments and Finite Element Analysis Simulations of Wire Arc Additive Manufacturing Technique. Metals and Materials International. The Korean Institute of Metals and Materials; 2022; Volume 28, pp. 54–111.
19. Ivántabernero, Paskual A, Álvarez P, Suárez A. Study on Arc Welding Processes for High Deposition Rate Additive Manufacturing. Procedia CIRP. 2018; Volume 68, pp. 358–62.
20. Shukla P, Dash B, Kiran DV, Bukkapatnam S. Arc behavior in wire arc additive manufacturing process. Procedia Manuf. 2020; Volume 48, pp. 725–9.
21. Zhao XF, Wimmer A, Zaeh MF. Experimental and simulative investigation of welding sequences on thermally induced distortions in wire arc additive manufacturing. Rapid Prototyp J. 2023; Volume 29, pp. 53–63.
22. Cambon C, Bendaoud I, Rouquette S, Soulié F. A WAAM benchmark: From process parameters to thermal effects on weld pool shape, microstructure and residual stresses. Mater Today Commun. 2022; Volume 33, pp. 104235.
23. Er C, Ganguly S, Xu X, Cabeza S, Coules H, Williams S. Study of residual stress and microstructural evolution in as-deposited and inter-pass rolled wire plus arc additively manufactured Inconel 718 alloy after ageing treatment. 2021; Volume 801, pp. 7346.
24. Hönnige JR, Colegrove PA, Ganguly S, Eimer E, Kabra S, Williams S. Control of Residual Stress and Distortion in Aluminium Wire + Arc Additive Manufacture with Rolling. Addit Manuf. 2018; Volume 22, pp. 775-783.
25. Schroepfer KWD, Wildenhain RS, Kannengiesser AHT, Hensel AKJ. Influence of the WAAM process and design aspects on residual stresses in high - strength structural steels. Weld World. 2023; Volume 67, pp. 987–96.
26. Geng R, Du J, Wei Z, Xu S, Ma N. Modelling and experimental observation of the deposition geometry and microstructure evolution of aluminum alloy fabricated by wire-arc additive manufacturing. J Manuf Process. 2021; Volume 64, pp. 369–78.
27. Klein T, Spoerk-Erdely P, Schneider-Broeskamp C, Oliveira JP, Abreu Faria G. Residual Stresses in a Wire and Arc-Directed Energy-Deposited Al–6Cu–Mn (ER2319) Alloy Determined by Energy-Dispersive High-Energy X-ray Diffraction. Metall Mater Trans A Phys Metall Mater Sci. 2024; Volume 55, pp. 736–44.
28. Ermakova A, Mehmanparast A, Ganguly S, Razavi N, Berto F. Investigation of mechanical and fracture properties of wire and arc additively manufactured low carbon steel components. Theor Appl Fract Mech. 2020;Volume 109, pp. 0–8.
29. Derekar KS. A review of wire arc additive manufacturing and advances in wire arc additive manufacturing of aluminium. Mater Sci Technol (United Kingdom). 2018; Volume 34, pp. 895–916.
30. Taşdemir A, Nohut S. An overview of wire arc additive manufacturing (WAAM) in shipbuilding industry. Ships Offshore Struct. 2020; Volume 16, pp. 1–18.
31. Williams SW, Martina F, Addison AC, Ding J, Pardal G, Colegrove P. Wire + Arc additive manufacturing. Mater Sci Technol (United Kingdom). 2016; Volume 32, pp. 641–7.
32. Müller J, Grabowski M, Müller C, Hensel J, Unglaub J, Thiele K, et al. Design and parameter identification of wire and arc additively manufactured (WAAM) steel bars for use in construction. Metals. 2019; Volume 9, pp. 725.

 doi:10.20944/preprints202405.0422.v1

33. Abbaszadeh M, Hönnige JR, Martina F, Neto L, Kashaev N, Colegrove P, et al. Numerical Investigation of the Effect of Rolling on the Localized Stress and Strain Induction for Wire + Arc Additive Manufactured Structures. J Mater Eng Perform. 2019; Volume 28, pp. 4931–42.
34. Song SS, Chen J, Quan G, Ye J, Zhao Y. Numerical analysis and design of concrete-filled wire arc additively manufactured steel tube under axial compression. Eng Struct. 2024; Volume 301, pp. 117294.
35. Wu Q, Mukherjee T, De A, DebRoy T. Residual stresses in wire-arc additive manufacturing - Hierarchy of influential variables. Addit Manuf. 2020; Volume 35. pp. 101355.
36. Ding D, Pan Z, Cuiuri D, Li H. Wire-feed additive manufacturing of metal components: technologies, developments and future interests. Int J Adv Manuf Technol. 2015; Volume 81, pp. 465–81.
37. Jafari D, Vaneker THJ, Gibson I. Wire and arc additive manufacturing : Opportunities and challenges to control the quality and accuracy of manufactured parts. Mater Des. 2021; Volume 202, pp. 109471.
38. Wu B, Pan Z, Chen G, Ding D, Yuan L, Cuiuri D, et al. Mitigation of thermal distortion in wire arc additively manufactured Ti6Al4V part using active interpass cooling. Sci Technol Weld Join. 2019; Volume 24, pp. 484–94.
39. Rozaimi M, Yusof F. Research challenges , quality control and monitoring strategy for Wire Arc Additive Manufacturing. J Mater Res Technol. 2023; Volume 24, pp. 2769–94.
40. Ahmad B, Zhang X, Guo H, Fitzpatrick ME, Neto LMSC, Williams S. Influence of Deposition Strategies on Residual Stress in Wire + Arc Additive Manufactured Titanium Ti-6Al-4V. Metals. 2022; Volume 12, pp. 253.
41. Schönegger S, Moschinger M, Enzinger N. Computational welding simulation of a plasma wire arc additive manufacturing process for high-strength steel. Eur J Mater. 2024; Volume 4, pp. 2297051.
42. Qvale P, Njaastad EB, Bræin T, Ren X. A fast simulation method for thermal management in wire arc additive manufacturing repair of a thin-walled structure. Int J Adv Manuf Technol. 2024; Volume 132, pp. 1573–1583.
43. Wang C, Suder W, Ding J, Williams S. The effect of wire size on high deposition rate wire and plasma arc additive manufacture of Ti-6Al-4V. 2021; Volume 288, pp. 1–22.
44. Gupta AK, Bansal H, Madan A. Study on CNC Wire Arc Additive Manufacturing process for Higher Deposition Rate and Mechanical Strength. 2022; Vlome 10, pp. 9695.
45. Agustinus Ananda P. WAAM Application for EPC Company. MATEC Web Conf. 2019; Volume 269, pp. 05002.
46. Li Y, Dong Z, Miao J, Liu H, Babkin A, Chang Y. Forming accuracy improvement in wire arc additive manufacturing (WAAM): a review. Rapid Prototyp J. 2022; Volume 29, pp. 1355- 2546.
47. Chaurasia M, Sinha MK. Investigations on Process Parameters of Wire Arc Additive Manufacturing (WAAM): A Review. Lect Notes Mech Eng. 2021; pp. 845–53.
48. Gowthaman PS, Jeyakumar S, Sarathchandra D. Effect of Heat Input on Microstructure and Mechanical Properties of 316L Stainless Steel Fabricated by Wire Arc Additive Manufacturing. J Mater Eng Perform. 2023.
49. Tomar B, Shiva S, Nath T. A review on wire arc additive manufacturing: Processing parameters, defects, quality improvement and recent advances. Mater Today Commun. 2022; Volume 31, pp. 103739.
50. Voropaev A, Korsmik R, Tsibulsky I. Features of filler wire melting and transferring in wire-arc additive manufacturing of metal workpieces. Materials. 2021; Volume 14, pp. 5077.
51. Chen C, He H, Zhou S, Lian G, Huang X, Feng M. Prediction of multi-bead profile of robotic wire and arc additive manufactured components recursively using axisymmetric drop shape analysis. Virtual Phys Prototyp. 2023; Volume 18, pp. 1–24.
52. Ayed A, Valencia A, Bras G, Bernard H, Michaud P, Balcaen Y, et al. Effects of WAAM Process Parameters on Metallurgical and Mechanical Properties of Ti-6Al-4V Deposits. Lect Notes Mech Eng. 2020; pp. 26–35.
53. Le VT, Si D, Khoa T, Paris H. Engineering Science and Technology , an International Journal Wire and arc additive manufacturing of 308L stainless steel components : Optimization of processing parameters and material properties. Eng Sci Technol an Int J. 2021; Volume 24, pp. 1015–26.
54. Lin Z, Goulas C, Ya W, Hermans MJM. Microstructure and mechanical properties of medium carbon steel deposits obtained via wire and arc additive manufacturing using metal-cored wire. Metals. 2019; Volume 9, pp. 673.
55. Song GH, Lee CM, Kim DH. Investigation of path planning to reduce height errors of intersection parts in wire-arc additive manufacturing. Materials. 2021; Volume 14, pp. 1–15.
56. Zhou Z, Shen H, Liu B, Du W, Jin J, Lin J. Residual thermal stress prediction for continuous tool-paths in wire-arc additive manufacturing: a three-level data-driven method. Virtual Phys Prototyp. 2022; Volume 17, pp. 105–24.
57. Guo C, Li G, Li S, Hu X, Lu H, Li X, et al. Additive manufacturing of Ni-based superalloys: Residual stress, mechanisms of crack formation and strategies for crack inhibition. Nano Mater Sci. 2023; Volume 5, pp. 53–77.

 doi:10.20944/preprints202405.0422.v1

58. Scotti FM, Teixeira FR, Silva LJ da, de Araújo DB, Reis RP, Scotti A. Thermal management in WAAM through the CMT Advanced process and an active cooling technique. J Manuf Process. 2020; Volume 57, pp. 23–35.
59. Ahsan MRU, Tanvir ANM, Ross T, Elsawy A, Oh MS, Kim DB. Fabrication of bimetallic additively manufactured structure (BAMS) of low carbon steel and 316L austenitic stainless steel with wire + arc additive manufacturing. Rapid Prototyp J. 2020; Volume 26, pp. 519–30.
60. Wu Q, Ma Z, Chen G, Liu C, Ma D, Ma S. Obtaining fine microstructure and unsupported overhangs by low heat input pulse arc additive manufacturing. J Manuf Process. 2017; Volume 27, pp. 198–206.
61. Doumenc G, Couturier L, Courant B, Paillard P, Benoit A, Gautron E, et al. Investigation of microstructure , hardness and residual stresses of wire and arc additive manufactured 6061 aluminium alloy To cite this version : HAL Id : hal-03827007. Materialia. 2022; Volume 25, pp. 101520.
62. Tröger J alexander, Hartmann S, Treutler K, Potschka A, Wesling V. Simulation-based process parameter optimization for wire arc additive manufacturing. Prog Addit Manuf. 2024.
63. Nagallapati V, Khare VK, Sharma A, Simhambhatla S. Active and Passive Thermal Management in Wire Arc Additive Manufacturing. Metals. 2023; Volume 13, pp. 682.
64. Ahsan MRU, Seo GJ, Fan X, Liaw PK, Motaman S, Haase C, et al. Effects of process parameters on bead shape, microstructure, and mechanical properties in wire + arc additive manufacturing of Al0.1CoCrFeNi high-entropy alloy. J Manuf Process. 2021;Volume 68, pp. 1314–27.
65. He T, Yu S, Shi Y, Huang A. Forming and mechanical properties of wire arc additive manufacture for marine propeller bracket. J Manuf Process. 2020; Volume 52, pp. 96–105.
66. Su C, Chen X, Gao C, Wang Y. Effect of heat input on microstructure and mechanical properties of Al-Mg alloys fabricated by WAAM. Appl Surf Sci. 2019; Volume 486, pp. 431–40.
67. Scharf-Wildenhain R, Haelsig A, Hensel J, Wandtke K, Schroepfer D, Kromm A, et al. Influence of Heat Control on Properties and Residual Stresses of Additive-Welded High-Strength Steel Components. Metals. 2022; Volume 12, pp. 951.
68. Javadi Y, Smith MC, Abburi Venkata K, Naveed N, Forsey AN, Francis JA, et al. Residual stress measurement round robin on an electron beam welded joint between austenitic stainless steel 316L(N) and ferritic steel P91. Int J Press Vessel Pip. 2017; Volume 154, pp. 41–57.
69. Saleh B, Fathi R, Tian Y, Jinghua NR, Aibin J. Fundamentals and advances of wire arc additive manufacturing : materials , process parameters , potential applications , and future trends. Archives of Civil and Mechanical Engineering. Springer London; 2023; Volume 23, pp. 1–71.
70. Rosli NA, Alkahari MR, bin Abdollah MF, Maidin S, Ramli FR, Herawan SG. Review on effect of heat input for wire arc additive manufacturing process. J Mater Res Technol. 2021; Volume 11, pp. 2127–45.
71. Liew J, Li Z, Alkahari MR, Ana N, Rosli B, Hasan R. Review of Wire Arc Additive Manufacturing for 3D Metal Printing Review of Wire Arc Additive Manufacturing for 3D Metal Printing. 2019; Volume 13, pp. 346-353. .
72. Woo W, Kim DK, Kingston EJ, Luzin V, Salvemini F, Hill MR. Effect of interlayers and scanning strategies on through-thickness residual stress distributions in additive manufactured ferritic-austenitic steel structure. Mater Sci Eng A. 2019; Volume 744, pp. 618–29.
73. Geng H, Li J, Gao J, Lin X. Theoretical model of residual stress and warpage for wire and arc additive manufacturing stiffened panels. Metals. 2020; Volume 10, pp. 666.
74. Rouquette S, Cambon C, Bendaoud I, Soulié F, Rouquette S, Cambon C, et al. Residual stresses in ss316l specimens after deposition of melted filler wire. ICRS11 11th Int Conf Residual Stress - Nancy – Fr – 27-30th March 2022.
75. Kumaran M, Senthilkumar V, Justus Panicke CT, Shishir R. Investigating the residual stress in additive manufacturing of repair work by directed energy deposition process on SS316L hot rolled steel substrate. Mater Today Proc. 2021; Volume 47, pp. 4475–8.
76. Mishurova T, Sydow B, Thiede T, Sizova I, Ulbricht A, Bambach M, et al. Residual stress and microstructure of a Ti-6Al-4V wire arc additive manufacturing hybrid demonstrator. Metals . 2020; Volume 10, pp. 701.
77. Martina F, Roy MJ, Szost BA, Terzi S, Colegrove PA, Williams SW, et al. Residual stress of as-deposited and rolled wire + arc additive manufacturing Ti – 6Al – 4V components. 2016; Volume 32, pp. 1439–48.
78. Liu C, Lin C, Wang J, Wang J, Yan L, Luo Y, et al. Residual stress distributions in thick specimens excavated from a large circular wire+arc additive manufacturing mockup. J Manuf Process. 2020; Volume 56, pp. 474–81.
79. Yang Y, Jin X, Liu C, Xiao M, Lu J, Fan H, et al. Residual stress, mechanical properties, and grain morphology of Ti-6Al-4V alloy produced by ultrasonic impact treatment assisted wire and arc additive manufacturing. Metals. 2018; Volume 8, pp.934.
80. Boruah D, Dewagtere N, Ahmad B, Nunes R, Tacq J, Zhang X, et al. Digital Image Correlation for Measuring Full-Field Residual Stresses in Wire and Arc Additive Manufactured Components. Materials. 2023; Volume 16, pp. 1702.

81. Steel S, Microstructure C. Wire Arc Additive Manufactured Mild Steel and Austenitic Properties and Residual Stresses. 2022.
82. Gao L, Chuang AC, Kenesei P, Ren Z, Balderson L, Sun T. An operando synchrotron study on the effect of wire melting state on solidification microstructures of Inconel 718 in wire-laser directed energy deposition. Int J Mach Tools Manuf. 2024; Volume 194, pp. 104089.
83. Robin IK, Sprouster DJ, Sridharan N, Snead LL, Zinkle SJ. Synchrotron based investigation of anisotropy and microstructure of wire arc additive manufactured Grade 91 steel. J Mater Res Technol. 2024; Volume 29, pp. 5010–21.
84. Kumar V, Mandal A. Parametric study and characterization of wire arc additive manufactured steel structures. 2021; Volume 115, pp. 1723–33.
85. Saleh B, Fathi R, Tian Y, Radhika N, Jiang J, Ma A. Fundamentals and advances of wire arc additive manufacturing: materials, process parameters, potential applications, and future trends. Archives of Civil and Mechanical Engineering. Springer London; 2023.
86. Shen C, Reid M, Liss KD, Pan Z, Ma Y, Cuiuri D, et al. Neutron diffraction residual stress determinations in Fe3Al based iron aluminide components fabricated using wire-arc additive manufacturing (WAAM). Addit Manuf. 2019; Volume 29, pp. 100774.
87. Rouquette S, Cambon C, Bendaoud I, Cabeza S, Soulié F. Effect of Layer Addition on Residual Stresses of Wire Arc Additive Manufactured Stainless Steel Specimens. J Manuf Sci Eng. 2024; Volume 146, pp. 1-12.
88. Rodrigues TA, Cipriano Farias FW, Zhang K, Shamsolhodaei A, Shen J, Zhou N, et al. Wire and arc additive manufacturing of 316L stainless steel/Inconel 625 functionally graded material: Development and characterization. J Mater Res Technol. 2022; Volume 21, pp. 237–51.
89. Théodore J, Couturier L, Girault B, Cabeza S, Pirling T, Frapier R, et al. Relationship between microstructure, and residual strain and stress in stainless steels in-situ alloyed by double-wire arc additive manufacturing (D-WAAM) process. Materialia. 2023.
90. Manikandan MDBKM. Evaluation of Microstructure , Residual Stress , and Mechanical Properties in Different Planes of Wire + Arc Additive Manufactured Nickel - Based Superalloy. Met Mater Int. 2022; Volume 28, pp. 3033–56.
91. Sun J, Hensel J, Köhler M, Dilger K. Residual stress in wire and arc additively manufactured aluminum components. J Manuf Process. 2021; Volume 65, pp. 97–111.
92. Rodrigues TA, Cipriano Farias FW, Avila JA, Maawad E, Schell N, Santos TG, et al. Effect of heat treatments on Inconel 625 fabricated by wire and arc additive manufacturing: an in situ synchrotron X-ray diffraction analysis. Sci Technol Weld Join. 2023; Volume 28, pp. 534–9.
93. Wandtke K, Becker A, Schroepfer D, Kromm A, Kannengiesser T, Scharf-Wildenhain R, et al. Residual Stress Evolution during Slot Milling for Repair Welding and Wire Arc Additive Manufacturing of High-Strength Steel Components. Metals. 2024 Volume 14, pp. 82.
94. Wu Q, Mukherjee T, Liu C, Lu J, DebRoy T. Residual stresses and distortion in the patterned printing of titanium and nickel alloys. Addit Manuf. 2019; Volume 29, pp. 100808.
95. Han Y. A Finite Element Study of Wire Arc Additive Manufacturing of Aluminum Alloy. Appl Sci. 2024; Volume 14, pp. 810.
96. Khaled H, Abusalma J. Parametric Study of Residual Stresses in Wire and Arc Additive Manufactured Parts. 2020.
97. Saadatmand M, Talemi R. Study on the thermal cycle of wire arc additive manufactured (WAAM) carbon steel wall using numerical simulation. Frat ed Integrita Strutt. 2020; Volume 14, pp. 98–104.
98. Eisazadeh H, Achuthan A, Goldak JA, Aidun DK. Effect of material properties and mechanical tensioning load on residual stress formation in GTA 304-A36 dissimilar weld. J Mater Process Technol. 2015; Volume 222, pp. 344–55.
99. Nezamdost MR, Esfahani MRN, Hashemi SH, Mirbozorgi SA. Investigation of temperature and residual stresses field of submerged arc welding by finite element method and experiments. Int J Adv Manuf Technol. 2016; Volume 87, pp. 615–24.
100. Huang H, Ma N, Chen J, Feng Z, Murakawa H. Toward large-scale simulation of residual stress and distortion in wire and arc additive manufacturing. Addit Manuf. 2020.
101. Han YS. Wire Arc Additive Manufacturing: A Study of Process Parameters Using Multiphysics Simulations. Materials. 2023; Volume 16, pp. 7267.
102. Jia J, Zhao Y, Dong M, Wu A, Li Q. Numerical simulation on residual stress and deformation for WAAM parts of aluminum alloy based on temperature function method. China Weld (English Ed. 2020; Volume 29, pp. 1–8.
103. Feng, G.; Wang H. W, Y.; Deng, D.; Zhang J. Numerical Simulation of Residual Stress and Deformation in Wire Arc Additive Manufacturing. Crystals. 2022; Volume 12, pp. 803.
104. Graf M, Pradjadhiana KP, Hälsig A, Manurung YHP, Awiszus B. Numerical simulation of metallic wire arc additive manufacturing (WAAM). AIP Conf Proc. 2018; Volume 960, pp. 140010.

105. Ahmad SN, Manurung YHP, Mat MF, Minggu Z, Jaffar A, Pruller S, et al. FEM simulation procedure for distortion and residual stress analysis of wire arc additive manufacturing. IOP Conf Ser Mater Sci Eng. 2020; Volume 834, pp. 012083.
106. Cadiou S, Courtois M, Carin M, Berckmans W, Le masson P. 3D heat transfer, fluid flow and electromagnetic model for cold metal transfer wire arc additive manufacturing (Cmt-Waam). Addit Manuf. 2020; Volume 36, pp. 101541.
107. Drexler H, Haunreiter F, Raberger L, Reiter L, Hütter A, Enzinger N. Numerical Modeling of Distortions and Residual Stresses During Wire Arc Additive Manufacturing of an ER 5183 Alloy with Weaving Deposition. BHM Berg- und Hüttenmännische Monatshefte. 2024; Volume 169, pp. 38–47.
108. Bonifaz EA, Palomeque JS. A mechanical model in wire + Arc additive manufacturing process. Prog Addit Manuf. 2020; Volume 5, pp. 163–9.
109. Reyes-gordillo E, Gómez-ortega A, Morales-estrella R, Pérez-barrera J, Gonzalez-carmona J, Alvarado-orozco J. Effect of Cold Metal Transfer Parameters during Wire Arc Additive Manufacturing of Ti6Al4V Multi- layer Walls. 2022.
110. Silva WF. Evaluation of the properties of Inconel ® 625 preforms manufactured using WAAM technology. Res Sq. 2024; pp. 1–21.
111. Derekar KS, Addison A, Joshi SS, Zhang X, Lawrence J, Xu L, et al. Effect of pulsed metal inert gas (pulsed-MIG) and cold metal transfer (CMT) techniques on hydrogen dissolution in wire arc additive manufacturing (WAAM) of aluminium. Int J Adv Manuf Technol. 2020; Volume 107, pp. 311–31.
112. Rosli NA, Alkahari MR, Ramli FR, Sudin MN, Maidin S. Influence of Process Parameters in Wire and Arc Additive Manufacturing (WAAM) Process. J Mech Eng. 2020; Volume 17, pp. 69–78.
113. Derekar KS, Ahmad B, Zhang X, Joshi SS, Lawrence J, Xu L, et al. Effects of Process Variants on Residual Stresses in Wire Arc Additive Manufacturing of Aluminum Alloy 5183. J Manuf Sci Eng Trans ASME. 2022; Volume 144, pp. 1–13.
114. Yuan Q, Liu C, Wang W, Wang M. Residual stress distribution in a large specimen fabricated by wire-arc additive manufacturing. Sci Technol Weld Join. 2023; Volume 28, pp. 137–44.
115. Fu R, Tang S, Lu J, Cui Y, Li Z, Zhang H, et al. Hot-wire arc additive manufacturing of aluminum alloy with reduced porosity and high deposition rate. Mater Des . 2021; pp. 199109370.
116. Zhang C, Li Y, Gao M, Zeng X. Wire arc additive manufacturing of Al-6Mg alloy using variable polarity cold metal transfer arc as power source. Mater Sci Eng A. 2018; Volume 711, pp. 415–23.
117. Corbin DJ, Nassar AR, Reutzel EW, Kistler NA, Beese AM, Michaleris P. Impact of directed energy deposition parameters on mechanical distortion of laser deposited Ti-6Al-4V. Solid Free Fabr 2016 Proc 27th Annu Int Solid Free Fabr Symp - An Addit Manuf Conf SFF 2016.; pp. 670–9.
118. Xiong J, Lei Y, Li R. Finite element analysis and experimental validation of thermal behavior for thin-walled parts in GMAW-based additive manufacturing with various substrate preheating temperatures. Appl Therm Eng. 2017;1 Volume 26, pp. 43–52.
119. Zhao J, Quan G zheng, Zhang Y qing, Ma Y yao, Jiang L he, Dai W wei, et al. Influence of deposition path strategy on residual stress and deformation in weaving wire-arc additive manufacturing of disc parts. J Mater Res Technol. 2024; Volume 30, pp. 2242–56.
120. Ouellet T, Croteau M, Bois-Brochu A, Lévesque J. Wire Arc Additive Manufacturing of Aluminium Alloys †. Eng Proc. 2023; Volume 43, pp. 2–6.
121. Li JLZ, Alkahari MR, Rosli NAB, Hasan R, Sudin MN, Ramli FR. Review of wire arc additive manufacturing for 3d metal printing. Int J Autom Technol. 2019; Volume 13, pp. 346–53.
122. Zhang J, Wang X, Paddea S, Zhang X. Fatigue crack propagation behaviour in wire+arc additive manufactured Ti-6Al-4V: Effects of microstructure and residual stress. Mater Des. 2016; Volume 90, pp. 551–61.
123. Gu J, Gao M, Yang S, Bai J, Zhai Y, Ding J. Microstructure, defects, and mechanical properties of wire + arc additively manufactured Al[sbnd]Cu4.3-Mg1.5 alloy. Mater Des. 2020; Volume 186, pp. 108357.
124. Kindermann RM, Roy MJ, Morana R, Francis JA. Effects of microstructural heterogeneity and structural defects on the mechanical behaviour of wire + arc additively manufactured Inconel 718 components. Materials Science and Engineering A. 2022, Volume 839, pp. 142826.
125. Yildiz AS, Koc BI, Yilmaz O. Thermal behavior determination for wire arc additive manufacturing process. Procedia Manuf. 2020;Volume 54, pp. 233–7.
126. Ali Y, Henckell P, Hildebrand J, Reimann J, Bergmann JP, Barnikol-Oettler S, et al. On the Influence of Linear Energy/Heat Input Coefficient on Hardness and Weld Bead Geometry in Chromium-Rich Stringer GMAW Coatings. J Manuf Proces. 2022; Volume 15, pp. 6019.
127. Romanenko D, Prakash VJ, Kuhn T, Moeller C, Hintze W, Emmelmann C. Effect of DED process parameters on distortion and residual stress state of additively manufactured Ti-6Al-4V components during machining. Procedia CIRP. 2022; Volume 11, pp. 271–6.
128. Layer-by-layer model-based adaptive control for wire arc additive manufacturing of thin-wall structures. 2022; Volume 33, pp. 1165–80.

 doi:10.20944/preprints202405.0422.v1

129. Liu B, Lan J, Liu H, Chen X, Zhang X, Jiang Z, et al. The Effects of Processing Parameters during the Wire Arc Additive Manufacturing of 308L Stainless Steel on the Formation of a Thin-Walled Structure. Materials. 2024; Volume 17, pp. 1337.
130. Ali MH, Han YS. A Finite Element Analysis on the Effect of Scanning Pattern and Energy on Residual Stress and Deformation in Wire Arc Additive Manufacturing of EH36 Steel. Materials. 2023; Volume 16. pp. 4698.
131. Chen S, He T, Wu X, Lei G. Synergistic effect of carbides and residual strain on the mechanical behavior of Ni-17 Mo-7Cr superalloy made by wire-arc additive manufacturing. Mater Lett. 2021; Volume 287, pp. 129291.
132. Winczek J, Gucwa M, Makles K, Mičian M, Yadav A. The amount of heat input to the weld per unit length and per unit volume. IOP Conf Ser Mater Sci Eng. 2021; Volume 1199, pp. 012067.
133. Koli Y, Arora S, Ahmad S, Priya, Yuvaraj N, Khan ZA. Investigations and Multi-response Optimization of Wire Arc Additive Manufacturing Cold Metal Transfer Process Parameters for Fabrication of SS308L Samples. J Mater Eng Perform. 2023; Volume 32, pp. 2463–75.
134. Cambon C, Rouquette S, Bendaoud I, Bordreuil C, Wimpory R, Soulie F. Thermo-mechanical simulation of overlaid layers made with wire + arc additive manufacturing and GMAW-cold metal transfer. Weld World. 2020; Volume 64, pp. 1427–35.
135. Omiyale BO, Olugbade TO, Abioye TE, Farayibi PK. Wire arc additive manufacturing of aluminium alloys for aerospace and automotive applications: a review. Mater Sci Technol (United Kingdom). 2022; Volume 38, pp. 391–408.
136. Wang J, Pan Z, Carpenter K, Han J, Wang Z, Li H. Comparative study on crystallographic orientation, precipitation, phase transformation and mechanical response of Ni-rich NiTi alloy fabricated by WAAM at elevated substrate heating temperatures. Mater Sci Eng A. 2021; Volume 800, pp. 140307.
137. Ding J, Colegrove P, Martina F, Williams S, Wiktorowicz R, Palt MR. Development of a laminar flow local shielding device for wire + arc additive manufacture. J Mater Process Technol. 2015; Volume 226, pp. 99–105.
138. Tonelli L, Laghi V, Palermo M, Trombetti T, Ceschini L. AA5083 (Al–Mg) plates produced by wire-and-arc additive manufacturing: effect of specimen orientation on microstructure and tensile properties. Prog Addit Manuf. 2021; Volume 6, pp. 479–94.
139. Zhang C, Shen C, Hua X, Li F, Zhang Y, Zhu Y. Influence of wire-arc additive manufacturing path planning strategy on the residual stress status in one single buildup layer. Int J Adv Manuf Technol. 2020; Volume 111, pp. 797–806.
140. Pawlik J, Cieślik J, Bembenek M, Góral T, Kapayeva S, Kapkenova M. On the Influence of Linear Energy/Heat Input Coefficient on Hardness and Weld Bead Geometry in Chromium-Rich Stringer GMAW Coatings. Materials. 2022; Volume 15, pp. 6019.
141. Denlinger ER, Heigel JC, Michaleris P, Palmer TA. Effect of inter-layer dwell time on distortion and residual stress in additive manufacturing of titanium and nickel alloys. J Mater Process Technol. 2015; Volume 215, pp. 123–31.
142. Gudur S, Nagallapati V, Pawar S, Muvvala G, Simhambhatla S. A study on the effect of substrate heating and cooling on bead geometry in wire arc additive manufacturing and its correlation with cooling rate. Mater Today Proc. 2019; Volume 41, pp. 431–6.
143. Singh S, Jinoop AN, Tarun Kumar GTA, Palani IA, Paul CP, Prashanth KG. Effect of interlayer delay on the microstructure and mechanical properties of wire arc additive manufactured wall structures. Materials. 2021; Volume 14, pp. 4187.
144. Bermingham MJ, Nicastro L, Kent D, Chen Y, Dargusch MS. Optimising the mechanical properties of Ti-6Al-4V components produced by wire + arc additive manufacturing with post-process heat treatments. J Alloys Compd. 2018; Volume 753, pp. 247–55.
145. Kumar A, Maji K. Selection of Process Parameters for Near-Net Shape Deposition in Wire Arc Additive Manufacturing by Genetic Algorithm. J Mater Eng Perform. 2020; Volume 29, pp. 3334–52.
146. Ali Y, Henckell P, Hildebrand J, Reimann J, Bergmann JP, Barnikol-Oettler S. Wire arc additive manufacturing of hot work tool steel with CMT process. J Mater Process Technol. 2019; Volume 269, pp. 109–16.
147. Laghi V. Tensile properties and microstructural features of 304L austenitic stainless steel produced by wire-and-arc additive manufacturing. 2020; Volume 106, pp. 3693–705.
148. Dinovitzer M, Chen X, Laliberte J, Huang X, Frei H. Effect of wire and arc additive manufacturing (WAAM) process parameters on bead geometry and microstructure. Addit Manuf. 2019; Volume 26, pp. 138–46.
149. Naveen Srinivas M, Vimal KEK, Manikandan N, Sritharanandh G. Parametric optimization and multiple regression modelling for fabrication of aluminium alloy thin plate using wire arc additive manufacturing. Int J Interact Des Manuf. 2022;
150. Zavdoveev A, Pozniakov V, Baudin T, Kim HS, Klochkov I, Motrunich S, et al. Optimization of the pulsed arc welding parameters for wire arc additive manufacturing in austenitic steel applications. Int J Adv Manuf Technol. 2022; Volume 119, pp. 5175–93.

151. Lu X, Li MV, Yang H. Comparison of wire-arc and powder-laser additive manufacturing for IN718 superalloy: unified consideration for selecting process parameters based on volumetric energy density. Int J Adv Manuf Technol. 2021; Volume 114, pp. 1517–31.
152. Vora J, Pandey R, Dodiya P, Patel V, Khanna S, Vaghasia V, et al. Fabrication of Multi-Walled Structure through Parametric Study of Bead Geometries of GMAW-Based WAAM Process of SS309L. Materials. 2023; Volume 16, pp. 5147.
153. Athaib NH, Haleem AH, Al-Zubaidy B. A review of Wire Arc Additive Manufacturing (WAAM) of Aluminium Composite, Process, Classification, Advantages, Challenges, and Application. J Phys Conf Ser. 2021; Volume 1973, pp. 012083.
154. Scharf-Wildenhain R, Haelsig A, Hensel J, Wandtke K, Schroepfer D, Kannengiesser T. Heat control and design-related effects on the properties and welding stresses in WAAM components of high-strength structural steels. Weld World. 2023; Volume 67, pp. 955–65.
155. Zhang J, Zhang X, Wang X, Ding J, Traoré Y, Paddea S, et al. Crack path selection at the interface of wrought and wire + arc additive manufactured Ti-6Al-4V. Mater Des. 2016; Volume 104, pp. 365–75.
156. Yang YH, Guan ZP, Ma PK, Ren MW, Jia HL, Zhao P, et al. Wire arc additive manufacturing of a novel ATZM31 Mg alloy: Microstructure evolution and mechanical properties. J Magnes Alloy. 2023; Volume 10, pp. 44.
157. Koli Y, Yuvaraj N, Sivanandam A, Vipin. Control of humping phenomenon and analyzing mechanical properties of Al–Si wire-arc additive manufacturing fabricated samples using cold metal transfer process. Proc Inst Mech Eng Part C J Mech Eng Sci. 2022; Volume 236, pp. 984–96.
158. Jing Y, Fang X, Xi N, Chang T, Duan Y, Huang K. Improved tensile strength and fatigue properties of wire-arc additively manufactured 2319 aluminum alloy by surface laser shock peening. Mater Sci Eng A. 2023; Volume 864, pp. 144599.
159. Chi J, Cai Z, Wan Z, Zhang H, Chen Z, Li L, et al. Effects of heat treatment combined with laser shock peening on wire and arc additive manufactured Ti17 titanium alloy: Microstructures, residual stress and mechanical properties. Surf Coatings Technol. 2020; Volume 396, pp. 125908.
160. Sousa BM, Coelho FGF, Júnior GMM, de Oliveira HCP, da Silva NN. Thermal and microstructural analysis of intersections manufactured by wire arc additive manufacturing (WAAM). Weld World. 2024; pp. 1–26.
161. Ma D, Xu C, Sui S, Tian J, Guo C, Wu X, et al. Microstructure evolution and mechanical properties of wire arc additively manufactured Mg-Gd-Y-Zr alloy by post heat treatments. Virtual Phys Prototyp. 2023; Volume 18, pp. 1–22.
162. Szost BA, Terzi S, Martina F, Boisselier D, Prytuliak A, Pirling T, et al. A comparative study of additive manufacturing techniques: Residual stress and microstructural analysis of CLAD and WAAM printed Ti-6Al-4V components. Mater Des. 2016; Volume 89, pp. 559–67.
163. Kumar A, Maji K, Shrivastava A. Investigations on Deposition Geometry and Mechanical Properties of Wire Arc Additive Manufactured Inconel 625. Int J Precis Eng Manuf. 2023; Volume 24, pp. 1483–500.
164. Vazquez L, Rodriguez MN, Rodriguez I, Alvarez P. Influence of post-deposition heat treatments on the microstructure and tensile properties of ti-6al-4v parts manufactured by cmt-waam. Metals. 2021; Volume 11, pp. 1161.
165. Kindermann RM, Roy MJ, Morana R, Francis JA. Materials Science & Engineering A Effects of microstructural heterogeneity and structural defects on the mechanical behaviour of wire + arc additively manufactured Inconel 718 components. Mater Sci Eng A. 2022; Volume 839, pp. 42826.
166. Geng H, Li J, Xiong J, Lin X, Zhang F. Optimization of wire feed for GTAW based additive manufacturing. J Mater Process Technol. 2017; Volume 243, pp. 40–7.
167. Li R, Xiong J, Lei Y. Investigation on thermal stress evolution induced by wire and arc additive manufacturing for circular thin-walled parts. J Manuf Process. 2019; Volume 40, pp. 59–67.
168. Gupta, Neel Kamal, G, Ganesan, Siddhartha, Karade Shahu, Mehta, Avinash Kumar, KP, Karunakaran. Effect of Multiple Technologies on Minimizing the Residual Stresses in Additive Manufacturing. ICRS 11 - 11th Int Conf Residual Stress SF2M; IJL, Mar 2022, Nancy, Fr. 2022; pp. 040150.
169. Ali MH, Han YS. Effect of phase transformations on scanning strategy in waam fabrication. Materials. 2021; Volume 14,
170. Gornyakov V, Sun Y, Ding J, Williams S. Modelling and optimising hybrid process of wire arc additive manufacturing and high-pressure rolling. Mater Des. 2022; Volume 223, pp. 111121.
171. Lailatul Mufidah KT. Efficient modelling and evaluation of rolling for mitigation of residual stress and distortion in wire arc additive manufacturing. Cranfield.ac.uk. 2021; Volume 7, pp. 265.
172. Zhang T, Li H, Gong H, Ding J, Wu Y, Diao C, et al. Hybrid wire - arc additive manufacture and effect of rolling process on microstructure and tensile properties of Inconel 718. J Mater Process Technol. 2022; Volume 299, pp. 321-6.
173. Srivastava S, Garg RK, Sharma VS, Sachdeva A. Measurement and Mitigation of Residual Stress in Wire-Arc Additive Manufacturing: A Review of Macro-Scale Continuum Modelling Approach. Arch Comput Methods Eng. 2021; Volume 28, pp. 3491–515.

 doi:10.20944/preprints202405.0422.v1

174. Montevecchi F, Venturini G, Scippa A, Campatelli G. Finite Element Modelling of Wire-arc-additive-manufacturing Process. Procedia CIRP. 2016; Volume 55, pp. 109–14.
175. Bankong BD, Abioye TE, Olugbade TO, Zuhailawati H, Gbadeyan OO, Ogedengbe TI. Review of post-processing methods for high-quality wire arc additive manufacturing. Mater Sci Technol (United Kingdom). 2023; Volume 39, pp. 129–46.
176. Hönnige JR, Colegrove PA, Ahmad B, Fitzpatrick ME, Ganguly S, Lee TL, et al. Residual stress and texture control in Ti-6Al-4V wire + arc additively manufactured intersections by stress relief and rolling. Mater Des. 2018; Volume 150, pp. 193–205.
177. Li K, Klecka MA, Chen S, Xiong W. Wire-arc additive manufacturing and post-heat treatment optimization on microstructure and mechanical properties of Grade 91 steel. Addit Manuf. 2021.
178. Nie L, Wu Y, Gong H, Chen D, Guo X. Effect of shot peening on redistribution of residual stress field in friction stir welding of 2219 aluminum alloy. Materials. 2020; Volume 13, pp. 1–13.
179. Sun R, Li L, Zhu Y, Guo W, Peng P, Cong B, et al. Microstructure, residual stress and tensile properties control of wire-arc additive manufactured 2319 aluminum alloy with laser shock peening. J Alloys Compd. 2018; Volume 747, pp. 255–65.
180. Ermakova A, Razavi N, Cabeza S, Gadalinska E, Reid M, Paradowska A, et al. The effect of surface treatment and orientation on fatigue crack growth rate and residual stress distribution of wire arc additively manufactured low carbon steel components. J Mater Res Technol. 2023; Volume 24, pp. 2988–3004.
181. Ding Y, Muñiz-Lerma JA, Trask M, Chou S, Walker A, Brochu M. Microstructure and mechanical property considerations in additive manufacturing of aluminum alloys. MRS Bull. 2016; Volume 41, pp. 745–51.
182. Busachi A, Erkoyuncu J, Colegrove P, Martina F, Ding J. Designing a WAAM based manufacturing system for defence applications. Procedia CIRP. 2015; Volume 37, pp. 48–53.
183. Abusalma, H., Eisazadeh, H., Hejripour, F., Bunn, J., & Aidun D. Parametric study of residual stress formation in Wire and Arc Additive Manufacturing. J Manuf Process. 2022; Volume 75, pp. 863-876.
184. Kyvelou P, Huang C, Li J, Gardner L. Residual stresses in steel I-sections strengthened by wire arc additive manufacturing. Structures. 2024; Volume 60,
185. Wu B, Pan Z, Ding D, Cuiuri D, Li H, Xu J, et al. A review of the wire arc additive manufacturing of metals: properties, defects and quality improvement. J Manuf Process. 2018; Volume 35, pp. 127–39.
186. Colegrove PA, Donoghue J, Martina F, Gu J, Prangnell P, Hönnige J. Application of bulk deformation methods for microstructural and material property improvement and residual stress and distortion control in additively manufactured components. Scr Mater. 2017; Volume 135, pp. 111–8.
187. Karmuhilan M, Sood AK. Intelligent process model for bead geometry prediction in WAAM. Mater Today Proc. 2018; Volume 5, pp. 24005–13.
188. Tang S, Wang G, Huang C, Li R, Zhou S, Zhang H. Investigation, modeling and optimization of abnormal areas of weld beads in wire and arc additive manufacturing. Rapid Prototyp J. 2020; Volume 26, pp. 183–95.
189. Pawlik J, Cieślik J, Bembenek M, Góral T, Kapayeva S, Kapkenova M. On the Influence of Linear Energy/Heat Input Coefficient on Hardness and Weld Bead Geometry in Chromium-Rich Stringer GMAW Coatings. Materials. 2022; Volume 15, pp. 1–22.
190. Veiga F, Suárez A, Aldalur E, Bhujangrao T. Effect of the metal transfer mode on the symmetry of bead geometry in waam aluminum. Symmetry. 2021; Volume 13, pp. 1245.
191. Ding D, Pan Z, Cuiuri D, Li H. A multi-bead overlapping model for robotic wire and arc additive manufacturing (WAAM). Robot Comput Integr Manuf. 2015; Volume 31, pp. 101–10.
192. Geng H, Xiong J, Huang D, Lin X, Li J. A prediction model of layer geometrical size in wire and arc additive manufacture using response surface methodology. Int J Adv Manuf Technol. 2017; Volume 93, pp. 175–86.
193. Banaee SA, Kapil A, Marefat F, Sharma A. Generalised overlapping model for multi-material wire arc additive manufacturing (WAAM). Virtual Phys Prototyp. 2023; Volume 18, pp. 1–22.
194. Surovi NA, Soh GS. Acoustic feature based geometric defect identification in wire arc additive manufacturing. Virtual Phys Prototyp. 2023; Volume 18, pp. 1–19.
195. Zhao Y tao, Li W gang, Liu A. Optimization of geometry quality model for wire and arc additive manufacture based on adaptive multi-objective grey wolf algorithm. Soft Comput. 2020; Volume 24, pp. 17401–16.
196. Alomari Y, Birosz MT, Andó M. Part orientation optimization for Wire and Arc Additive Manufacturing process for convex and non-convex shapes. Sci Rep. 2023; Volume 13, pp. 2203.
197. Wani ZK, Abdullah AB. Bead Geometry Control in Wire Arc Additive Manufactured Profile - A Review. Pertanika J Sci Technol. 2024; Volume 32, pp. 917–42.
198. Vora J, Parikh N, Chaudhari R, Patel VK, Paramar H, Pimenov DY, et al. applied sciences Optimization of Bead Morphology for GMAW-Based Wire-Arc Metal-Cored Wires. 2022; Valome 12, pp. 1–18.
199. Wang C, Bai H, Ren C, Fang X, Lu B. A comprehensive prediction model of bead geometry in wire and arc additive manufacturing. J Phys Conf Ser. 2020; Valome 1624, pp. 1624.

 doi:10.20944/preprints202405.0422.v1

200. Chintala A, Tejaswi Kumar M, Sathishkumar M, Arivazhagan N, Manikandan M. Technology Development for Producing Inconel 625 in Aerospace Application Using Wire Arc Additive Manufacturing Process. J Mater Eng Perform. 2021; Valome 30, pp. 5333–41.
201. Hamrani A, Bouarab FZ, Agarwal A, Ju K, Akbarzadeh H. Advancements and applications of multiple wire processes in additive manufacturing: a comprehensive systematic review. Virtual Phys Prototyp. 2023; Valome 18, pp. 1–34.
202. Queguineur A, Rückert G, Cortial F, Hascoët JY. Evaluation of wire arc additive manufacturing for large-sized components in naval applications. Weld World. 2018; Valome 62, pp. 259–66.
203. Li J, Cui Q, Pang C, Xu P, Luo W, Li J. Integrated vehicle chassis fabricated by wire and arc additive manufacturing: structure generation, printing radian optimisation, and performance prediction. Virtual Phys Prototyp. 2024; Valome 19, pp. 1–22.
204. Singh SR, Khanna P. Wire arc additive manufacturing (WAAM): A new process to shape engineering materials. Mater Today Proc. 2021; Valome 44, pp. 118–28.
205. Vishnukumar M, Pramod R, Rajesh Kannan A. Wire arc additive manufacturing for repairing aluminium structures in marine applications. Mater Lett. 2021; Valome 299, pp. 130112.
206. Shah A, Aliyev R, Zeidler H, Krinke S. A Review of the Recent Developments and Challenges in Wire Arc Additive Manufacturing (WAAM) Process. J Manuf Mater Process. 2023; Valome 7, pp. 97.
207. Wire Arc Additive Manufacturing: Review on Recent Findings and Challenges in Industrial Applications and Materials Characterization. Metals. 2021; Volume 11, pp. 939.
208. Boţilă LN. Considerations regarding aluminum alloys used in the aeronautic/aerospace industry and use of wire arc additive manufacturing WAAM for their industrial applications. 2020; Valome 4, pp. 9–24.
209. Liu J, Xu Y, Ge Y, Hou Z, Chen S. Wire and arc additive manufacturing of metal components: a review of recent research developments. Int J Adv Manuf Technol. 2020; Valome 111, pp. 149–98.
210. Arana M, Ukar E, Rodriguez I, Aguilar D, Álvarez P. Influence of deposition strategy and heat treatment on mechanical properties and microstructure of 2319 aluminium WAAM components. Mater Des. 2022; Valome 221, pp. 110974.
211. Li H, Zhang Q, Chong C, Yap R, Tay K, Hang T, et al. Challenges associated with the wire arc additive manufacturing (WAAM) of Aluminum alloys. Mater Today Proc. 2019; Valome 221, pp. 6–20.
212. Zhao Y, Li F, Chen S, Lu Z. Unit block–based process planning strategy of WAAM for complex shell–shaped component. Int J Adv Manuf Technol. 2019; Valome 104, pp. 3915–27.
213. Pant H, Arora A, Gopakumar GS, Chadha U, Saeidi A, Patterson AE. Applications of wire arc additive manufacturing (WAAM) for aerospace component manufacturing. Int J Adv Manuf Technol. 2023; Valome 127, pp. 4995–5011.
214. Bachus NA, Strantza M, Clausen B, D'Elia CR, Hill MR, Ko JYP, et al. Novel bulk triaxial residual stress mapping in an additive manufactured bridge sample by coupling energy dispersive X-ray diffraction and contour method measurements. Addit Manuf. 2024; Valome 83, pp. 104070.
215. J.V. Gordon, C.V. Haden, H.F. Nied RPV and D. Fatigue crack growth anisotropy, texture and residual stress in austenitic steel made by wire and arc additive manufacturing. Mater Sci Eng A. 2018; Valome 115, pp. 60–6.